NTNU
Det skapende universitet

Compact Stars

Vegar Andreassen

Master i realfag
Innlevert: juni 2017
Hovedveileder: Jens Oluf Andersen, IFY

Norges teknisk-naturvitenskapelige universitet
Institutt for fysikk

Abstract

In this thesis we study the mass-radius and pressure-radius relations of white dwarfs and neutron stars. We derive the pressure and energy density in a non-interacting Fermi gas at $T = 0$, and construct several different equations of state. A comparison is made between different numerical algorithms, and a fourth order Runge-Kutta method is found to be the most suitable option. The Newtonian equations of stellar structure are derived, and then solved numerically to find a the mass-radius relation and maximum mass for white dwarfs. Good agreement with observational data is established. We derive the Tollman-Oppenheimer-Volkoff equation and solve them numerically to find the mass-radius relation and maximum mass for neutron stars. The maximum mass found appears to be significantly lower than expected. Finally the issue of stability and collapse is addressed.

Notation and Conventions

Metric The signature of the metric is (-, +, +, +)

Units SI units are used, except in the derivation of the Tollman-Oppenheimer-Volkoff equation, where natural units are used.

Acknowledgements

My friends at our cozy study hall deserve recognition for motivating me to work harder than I otherwise would have on this thesis - it wouldn't have been the same without you! Similarly, I extend heartfelt gratitude to my supervisor, Professor Jens Oluf Andersen, for his guidance and constructive criticism. I would also like to thank NTNU for accommodating me through the years.

Contents

1 Introduction

In 1916 the Estonian astronomer Ernst Öpik estimated the density of several binary stars, and found that one of them - the star which we today refer to as the white dwarf 40 Eridani B - had a density 25000 times greater than density of the sun. He thought that such a large density was an impossibility, and took the result as an indication that something was wrong with his assumptions.[1] He was not alone in this view - Arthur Eddington later said on the subject of the white dwarf Sirius B:[2]

> We learn about the stars by receiving and interpreting the messages which their light brings to us. The message of the Companion of Sirius when it was decoded ran: "I am composed of material 3,000 times denser than anything you have ever come across; a ton of my material would be a little nugget that you could put in a matchbox." What reply can one make to such a message? The reply which most of us made in 1914 was—"Shut up. Don't talk nonsense."

Today we know that in a star like our sun there is a balance between gravity pulling inwards, and fusion by-products pushing outwards. However, given time the nuclear fusion in the core of a star will stop. In a complicated process massive amounts of gas will be ejected out and away, while the core contracts, leaving a stellar remnant.[3] In the case of white dwarfs the exact composition of the core depends greatly upon the progenitor star. The heavier the star the hotter and denser the core, thus more readily fusing heavier elements, resulting in a white dwarf comparatively richer in heavy elements like carbon and oxygen; whereas a lighter star will not burn so hot, and its remains will consist of comparatively more helium. By contrast, neutron stars - remnants of stars heavy enough to continue fusion through iron - all share the same fate.[4]

In either case, the extremely dense core is now experiencing even greater gravitational forces, with no fusion fueled radiation pressure to counteract it. Yet both white dwarfs and neutron stars are stable. By which mechanisms are these compact stars stable against gravitational collapse? This question was answered with the advent of quantum mechanics - in particular with the formulation of the Pauli exclusion principle and the discovery of Fermi-Dirac statistics - fermions stubbornly refuse to be clumped too close together, and this simple fact can be used to explain much about the structure of compact stars. We will study this balance of power between gravity and the exclusion principle by deriving the stellar structure equations, and then using numerical methods to solve them.

When dealing with white dwarfs it is quite sufficient to consider only Newtonian gravity, but when we consider neutron stars it becomes necessary to employ the general relativistic equations of Einstein. We will model our compact star as a zero temperature non-interacting Fermi gas, and then improve upon our model by using successively more sophisticated numerical methods.

Figure 1: The Helix Nebula - a stellar remnant. (Courtesy of NASA)

2 Polytropic Equations of State

2.1 Gravitational Equilibrium

We begin by deriving a general result pertaining to the conditions inside a spherically symmetric star under the influence of its own gravity. Let us assume that there is some - as of yet unexplained - equal force but opposite force working to counteract gravity, so that the star is in hydrostatic equilibrium. Consider a thin shell at a radius r within the sphere in Figure 2, with thickness dr, density $\rho(r)$, and mass per unit area ρdr. If $g(r)$ is the gravitational acceleration felt at the radius r, then by Newton's second law there is a small gravitational force per unit area, $g\rho dr$, acting on the shell. We recall that force per unit area is the definition of pressure. Knowing this and our assumption of hydrostatic equilibrium, we may equate $g\rho dr$ to an infinitesimal pressure dP.

Given that the mass M contained within the spherical shell is

$$M(r) = \int_0^r \rho(r')4\pi r'^2 dr', \tag{1}$$

we have that the gravitational acceleration g is

$$g(r) = -GM(r)/r^2, \tag{2}$$

and that the pressure gradient dP/dr is

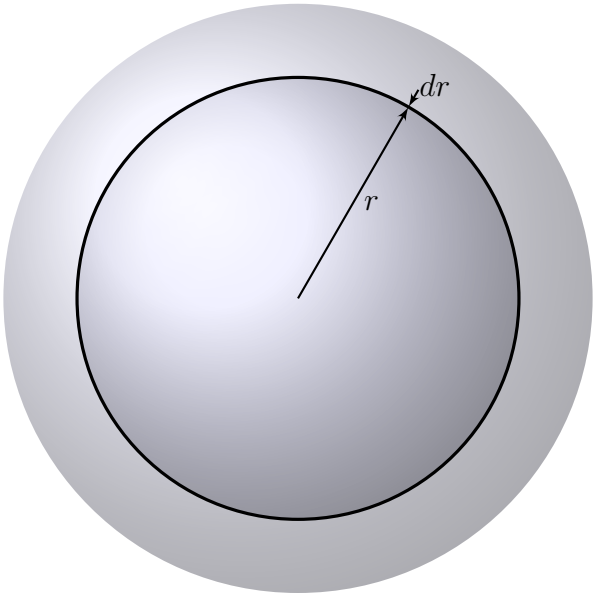

Figure 2: A spherical shell inside a star.

$$\frac{dP}{dr} = g\rho = -\frac{G\rho(r)M(r)}{r^2}. \tag{3}$$

Knowing that the mass M is a function of the density ρ and the radius r, one may effectively consider equation (3) a differential equation relating the pressure and density inside a star. This is important to note because it tells us that if we can find some additional relation between the pressure and the density, then it might be possible to solve equation (3) analytically. Failing that, one may find an approximate numerical solution.

2.2 The Pauli Exclusion Principle and the Fermi Gas

An equation relating pressure to density is commonly referred to as an equation of state, and the most well known among them is perhaps the ideal gas law. In this section we will consider the quantum analogue to the classical ideal gas, namely the ideal Fermi gas. The difference between the classical ideal gas and the Fermi ideal gas is that in the quantum case we take into account the fact that, per the Pauli exclusion principle, no two fermions ever occupy the same quantum mechanical state.

Assume that we have a cube with lengths l, whose properties allow electrons to move freely within the boundaries of the box, but to never escape from it. Furthermore we exclude all interparticle interactions from the potential:

$$V(x,y,z) = \begin{cases} 0, & 0 < x,y,z < l \\ \infty, & otherwise. \end{cases} \tag{4}$$

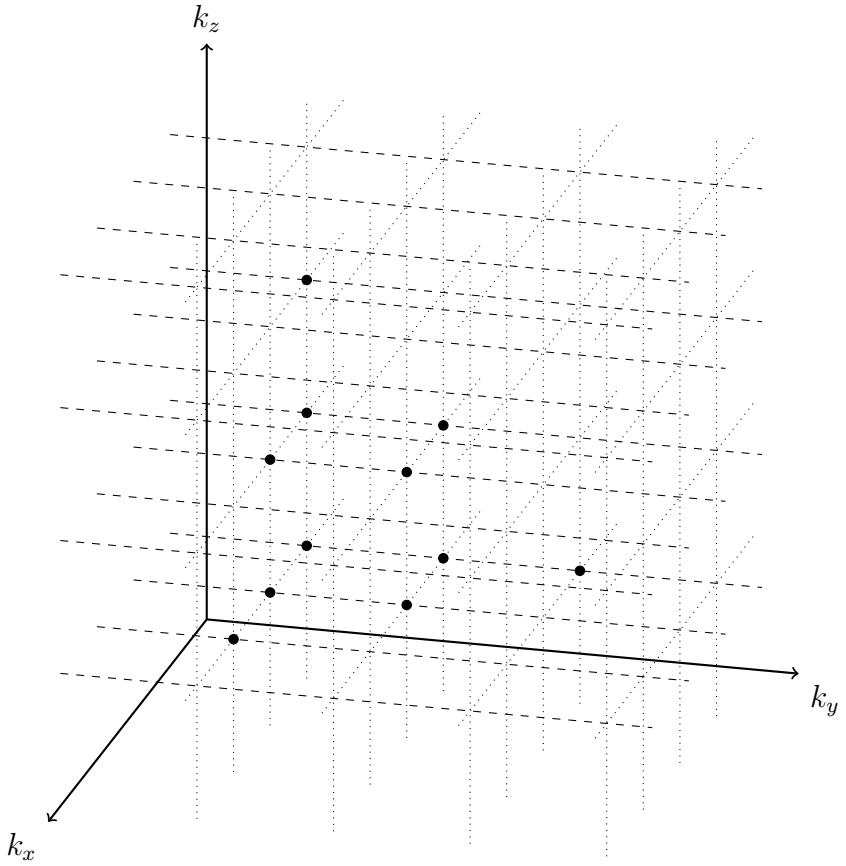

Figure 3: Allowed electron positions in k-space.

By separating the variables and applying the boundary conditions one finds the allowed momenta[5]

$$\begin{aligned} p^2 &= \hbar^2 k^2 \\ &= \hbar^2 (k_x^2 + k_y^2 + k_z^2) \\ &\equiv \hbar^2 \left(\frac{n_x^2 \pi^2}{l^2} + \frac{n_y^2 \pi^2}{l^2} + \frac{n_z^2 \pi^2}{l^2} \right), \end{aligned} \tag{5}$$

where each n is an integer, and k is the magnitude of the wave vector. The k_x, k_y and k_z in equation (5) represent different quantum numbers, and since no two electrons can occupy the same state, we have that each new electron put into the box needs a different set of these quantum numbers. A common way to visualize the allowed momenta is to imagine a three dimensional k-space with axes k_x, k_y and k_z, where the electrons can only occupy positions at the intersections $\frac{\pi}{l}(1,1,1)$, $\frac{\pi}{l}(1,1,2)$, $\frac{\pi}{l}(1,2,1)$, and so on.

Inserting equation (5) into the relativistic energy momentum relation

$$E^2 = p^2 c^2 + (mc)^2 c^2, \tag{6}$$

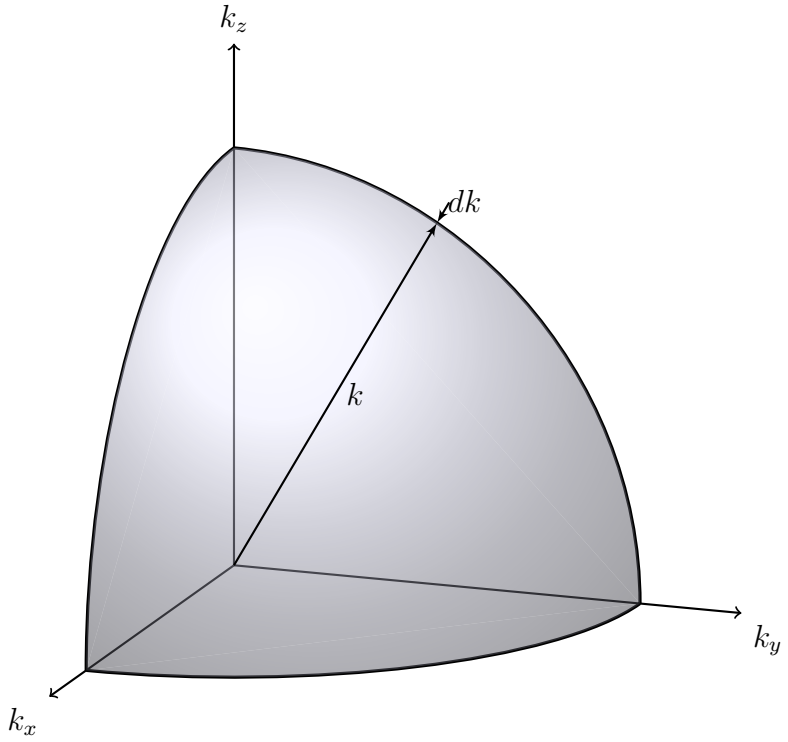

Figure 4: A visualization of k-space in the large N-limit.

yields

$$E^2 = (\hbar k)^2 c^2 + (mc)^2 c^2. \tag{7}$$

This tells us that electrons with higher k-values have higher energy, and taken together with the principle that the most probable physical configurations are those where the energy is at a minimum, we can infer that electrons are most likely to be found as close to the origin in k-space as they can be without violating the exclusion principle. So for large numbers of electrons the most probable configurations in k-space would look as depicted in Figure 4, since if we assume that the thermal energy in the star is low, then any electrons located outside the shaded region in Figure 4 will quickly settle down into more energetically favorable positions. The exclusion principle essentially causes the electrons to fill up one spherical layer after another. We can use this knowledge about the electron configuration in k-space to relate the maximum value of k to the number of electrons N, which in turn will allow us to find the electron density N/V.

As seen from Figure 3 the volume of one 'cell' in k-space is $\pi^3/l^3 = \pi^3/V$. If N is large then this is to very good approximation the volume per two electrons in k-space, since we can fit one spin up and one spin down electron into each cell due to the Pauli exclusion principle. So given some maximum value k_F we can say that the total volume taken up by all the electrons in k-space is

$$N\frac{\pi^3}{2V} = \frac{1}{8}\left(\frac{4\pi}{3}k_F^3\right). \tag{8}$$

By equation (5) we may then express the maximum momentum, p_F, of a single electron - known as the Fermi momentum - as a function of the electron number density $n_e = N/V$

$$p_F^3 = 3\pi^2\hbar^3 n_e, \tag{9}$$

and the corresponding Fermi energy as

$$E_F^2 = (3\pi^2 n_e)^{2/3}\hbar^2c^2 + (m_ec)^2c^2. \tag{10}$$

If we go to the continuum limit in our octant of k-space then a single spherical shell of thickness dk contains a volume $\frac{1}{8}(4\pi k^2)dk$. Earlier we noted that each state occupies a volume $\frac{\pi^3}{2V}$, so in any given shell the density of states is

$$\frac{1}{8}(4\pi k^2)\frac{2V}{\pi^3}dk = \frac{V}{\pi^2}k^2dk. \tag{11}$$

Each of these states carry an energy $[(\hbar k)^2c^2 + (m_ec)^2c^2]^{1/2}$, so the energy of a shell of electrons is

$$dE_e = [k^2\hbar^2c^2 + (m_ec)^2c^2]^{1/2}\frac{V}{\pi^2}k^2dk, \tag{12}$$

and hence the total energy of the electrons is

$$E_e = \frac{V}{\pi^2}\int_0^{k_F}[k^2\hbar^2c^2 + (m_ec)^2c^2]^{1/2}k^2dk. \tag{13}$$

Dividing by V and substituting $u = \frac{k\hbar}{m_ec}$ and the relativity parameter $u_F = \frac{k_F\hbar}{m_ec}$ yields the total energy density of the electrons

$$\epsilon_e = \frac{1}{\pi^2}\int_0^{u_F}\frac{u^2}{\hbar^2}(m_ec)^2\left[\frac{u^2}{\hbar^2}(m_ec)^2\hbar^2c^2 + (m_ec)^2c^2\right]^{1/2}\frac{m_ec}{\hbar}du \tag{14a}$$

$$= \frac{m_e^4c^5}{\pi^2\hbar^3}\int_0^{u_F}(u^2+1)^{1/2}u^2du \tag{14b}$$

$$= \frac{m_e^4c^5}{8\pi^2\hbar^3}\left[(2u_F^3 + u_F)(1+u_F^2)^{1/2} - \sinh^{-1}(u_F)\right]. \tag{14c}$$

A special case of this result is when the electrons are non-relativistic, so that $k_F\hbar \ll m_ec$. Then u_F is always small, and the dominant term in equation (14b) is

$$\epsilon_e = \frac{m_e^4c^5}{\pi^2\hbar^3}\int_0^{u_F}u^2du = \frac{m_ec^2}{3\pi^2}k_F^3. \tag{15}$$

If we then re-write equation (9) as $k_F^3 = 3\pi^2 n_e$, we find that the sum of the energy densities from the electrons and nucleons is

$$\epsilon = \epsilon_N + \epsilon_e = \frac{A}{Z} n_e m_N c^2 + n_e m_e c^2, \tag{16}$$

which is exactly what you would expect from non-relativistic matter - the energy density is the number density times the mass energy. Furthermore, since the mass of the nucleons is three orders of magnitude larger than the mass of the electron we can to good approximation write $\epsilon = \frac{A}{Z} n_e m_N c^2$, which can be rewritten as

$$\epsilon = \frac{A}{Z} \frac{m_n c^2}{3\pi^2} k_F^3. \tag{17}$$

This then is half of the relationship between pressure and density that we need in order to solve equation (3), and in Appendix A we derive the other half - the relationship between the pressure and the Fermi momentum k_F,

$$P = \frac{m_e^4 c^5}{3\pi^2 \hbar^3} \int_0^{u_F} (u^2 + 1)^{-1/2} u^4 du, \tag{18}$$

which has the analytic solution

$$P = \frac{m_e^4 c^5}{24\pi^2 \hbar^3} \left[(2u_F^3 - 3u_F)(1 + u_F^2)^{1/2} + 3 \sinh^{-1}(u_F) \right]. \tag{19}$$

Again we consider the case of non-relativistic electrons, $p_F \ll m_e c$. Then as before u_F is small, and the dominant term in equation (18) is

$$P = \frac{m_e^4 c^5}{3\pi^2 \hbar^3} \int_0^{u_F} u^4 du = \frac{\hbar^2}{15\pi^2 m_e} k_F^5. \tag{20}$$

2.3 Relativistic and Non-Relativistic Polytropes

Inserting equation (17) gives the relationship between the energy density $\epsilon = \rho c^2$ and the pressure P in the non-relativistic case

$$P = \frac{\hbar^2}{15\pi^2 m_e} \left(\frac{3\pi^2}{m_N c^2} \frac{Z}{A} \right)^{5/3} \epsilon^{5/3} \equiv K_{\rm NR} \epsilon^{5/3}, \tag{21}$$

where we have combined all all the numerical factors into a single parameter. Having already done the calculation for the non-relativistic case, it is straightforward to use equations (14) and (18) to show that in the case of relativistic electrons, $p_F \gg m_e c$, the energy density of the electrons is

$$\epsilon_e = \frac{\hbar c}{4\pi^2} k_F^4, \tag{22}$$

and the contribution to the pressure from the electrons is

$$P = \frac{\hbar c}{12\pi^2} k_F^4. \tag{23}$$

Using the identities $k_F^3 = 3\pi^2 n_e$ and $u_F = \frac{k_F \hbar}{m_e c}$ we can write the total energy density as

$$\epsilon = \epsilon_N + \epsilon_e = \frac{A}{Z} n_e m_N c^2 + u_F \frac{3}{4} n_e m_e c^2, \tag{24}$$

where we have again assumed that the energy density of the nucleons is a constant.

Comparing equation (24) with the analogous non-relativistic expression in equation (16) reveals a quadratic dependence upon the relativity parameter u_F, and through it the Fermi momentum k_F. We can estimate when the contribution of the electrons to the energy density becomes relevant by looking at a pared down version of equation (24)

$$\frac{\epsilon}{n_e c^2} = \frac{A}{Z} m_N + u_F \frac{3}{4} m_e \tag{25}$$

Given that the nucleons are roughly 2000 times as massive as the electron, and that the ration of protons to nucleons is typically close to 1/2, we conclude that for the electrons to contribute one percent of the total energy density, the relativity parameter u_F must be equal to 5.5. Knowing this one can use the approximation that electrons do not contribute to the energy density, and as in the non-relativistic case we write $\epsilon = \frac{A}{Z} n_e m_N c^2$. Using this approximation gives us a relationship between the energy density ϵ and the pressure P in the relativistic case

$$P = \frac{\hbar c}{12\pi^2} \left(\frac{3\pi^2}{m_N c^2} \frac{Z}{A} \right)^{4/3} \epsilon^{4/3} \equiv K_{\mathrm{R}} \epsilon^{4/3}. \tag{26}$$

However, we keep in mind that for sufficiently large values of the relativity parameter u_F one may no longer ignore the contribute of the electrons to the energy density.

Collectively we call equations of the form $P = K\rho^\gamma$ - or, as seen in equations (21) and (26), $P = K\epsilon^\gamma$ - polytropes, where γ is known as the polytropic exponent. Combining the general form of a polytropic equation with the differential forms of the equations of stellar structure, (1) and (3), yields a set of coupled differential equations

$$P' = -\frac{GM}{c^2 r^2} \left(\frac{P}{K} \right)^{1/\gamma}, \tag{27a}$$

$$M' = 4\pi \frac{r^2}{c^2} \left(\frac{P}{K} \right)^{1/\gamma}, \tag{27b}$$

which, given suitable boundary conditions, may be solved to give the pressure P and the mass M as functions of the radius r. We shall attempt a numerical solution, but before that, we will rescale the above expressions, make them dimensionless, and combine some of the numerical factors.

3 White Dwarfs

3.1 Scaling and Dimensionless Equations

In general one may scale an equation by dividing all dimensionful variables by a constant of the same dimension, often refered to as 'the scale'. For instance, we may divide every mass term by a kilogram, a metric tonne, or - more customarily - by a relevant scale of the problem, such as the mass of the sun[6]. One may also do as we did when integrating over momenta in equation (14), and scale using a parameter created by combining several dimensionful constants. Restating the problem in a dimensionless form typically helps us to identify any fundamental scales of the problem, and to pinpoint when a parameter is small or large.

Taking a cue from equations (14b) and (18) we pick

$$\epsilon_0 = \frac{m_N^4 c^5}{3\pi^2\hbar^3} = 5.46 \cdot 10^{35}\ J/m^3, \tag{28}$$

to be our energy density scale, but note that this is but one reasonable choice among many - for instance one might choose m_e as opposed to m_N. The scaled pressure and energy density are then defined by

$$P = \epsilon_0 \bar{P}, \tag{29}$$

$$\epsilon = \epsilon_0 \bar{\epsilon}. \tag{30}$$

This turns the polytropes into dimensionless equations of the form

$$\bar{P} = \bar{K}\bar{\epsilon}^\gamma, \tag{31}$$

where the factor $\bar{K} = K\epsilon_0^{\gamma-1}$ becomes the - now dimensionless - constant of proportionality. Similarly we scale the mass by the mass of the sun, $M_\odot$, and introduce the constant $R_0 \equiv GM_\odot/c^2$, so that

$$M = M_\odot \bar{M}. \tag{32}$$

Putting it all together transforms equations (27) into

$$\bar{P}' = -\frac{\alpha \bar{P}^{1/\gamma}\bar{M}}{r^2}, \tag{33a}$$

$$\bar{M}' = \beta \bar{P}^{1/\gamma} r^2, \tag{33b}$$

where the constants α and β are, respectively

$$\alpha = \frac{GM_\odot}{c^2 K^{1/\gamma}\epsilon_0^{1-1/\gamma}}, \tag{34}$$

and

$$\beta = \frac{4\pi\epsilon_0^{1/\gamma}}{M_\odot c^2 K^{1/\gamma}}. \tag{35}$$

3.2 Comparison of Numerical Methods

Later on we shall employ more sophisticated algorithms, but for a first approximation we combine the coupled differential equations in (33) with the non-relativistic polytrope in equation (21) and solve them in a straightforward way by repeat application of the first order finite central difference method

$$P'(r) = \frac{P(r+dr) - P(r-dr)}{2dr} \Rightarrow \tag{36}$$

$$P(r+dr) = 2drP'(r) + P(r-dr), \tag{37}$$

in order to get a basic understanding of the shape of the solution. One may use some combination of solid state physics and astronomical observations of mass and radius to estimate the central pressure ρ_c at the center of a white dwarf, and with each step of the algorithm work our way outward to the edge, where we expect the pressure to tend towards zero. A typical white dwarf might have an average density on the order of $4.0 \cdot 10^8$ kg/m^3[7]. With the choice of scale in equation (30), this density would be equivalent to a dimensionless energy density of $6.6 \cdot 10^{-11}$. Using equations (21) and (26) we get an average pressure on the order of $6.0 \cdot 10^{20}$ and $1.3 \cdot 10^{21}$ - under the assumption of non-relativistic and relativistic polytrope, respectively.

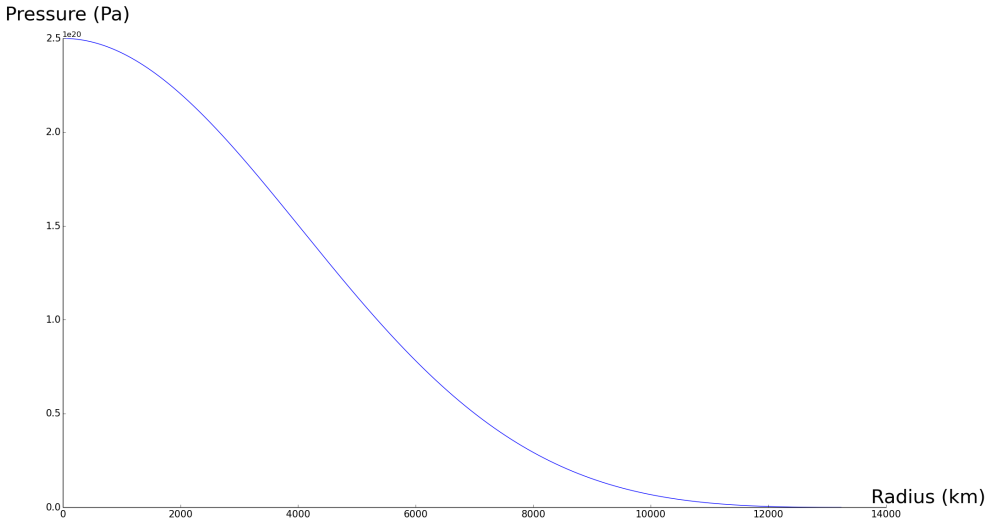

Figure 5: Pressure as a function of radius for a white dwarf star, as predicted by a first order finite difference solution of a non-relativistic polytrope - $\gamma = 5/3$, starting with a central pressure of $2.5 \cdot 10^{20}$ Pa.

Using a very conservative estimate of $2.5 \cdot 10^{20}$ Pa for the central pressure, we have in Figure 5 used the first order finite difference approach starting from the center, and it paints a clear picture. We also performed the integration for $2.5 \cdot 10^{21}$ Pa and $2.5 \cdot 10^{22}$

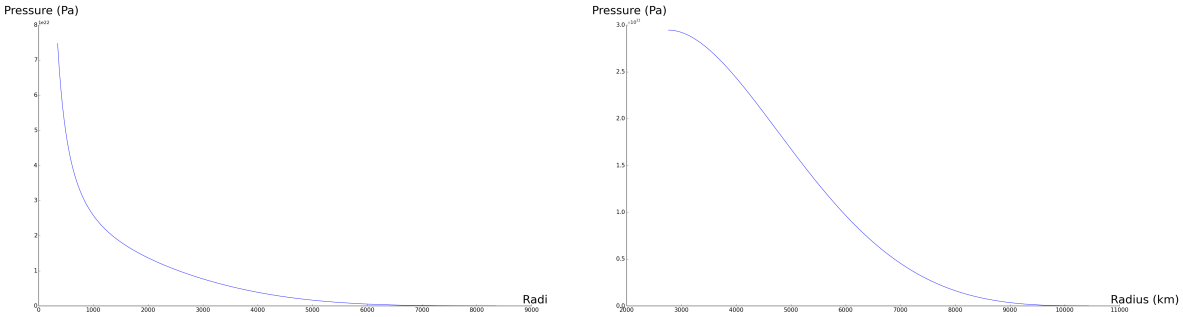

(a) Stopped at $r \approx 500$km, $M > 0$ (b) Algorithm ended at $r \approx 3000$km, $M = 0$

Figure 6: Pressure as a function of radius for a white dwarf star, as predicted by a first order finite difference solution of a non-relativistic polytrope, starting at the edge of the star.

Pa, and found that the integration traces out the same curve, but with a smaller final radius. Conversely, decreasing the central pressure increases the radius.

In Figure 6 we attempted an alternative approach, and assumed that the star has some radius R and total mass M - corresponding to those of the white dwarf Procyon B - and worked inward until either the mass or the radius became zero. In hindsight one might have predicted that this approach was too naive. Looking at Figure 6a we see that while the solution appears similar for large values of r, there is no turning point in the graph and it eventually blows up - which is why we cut off the graph at $r \approx 500$km, as it would otherwise continue upwards for roughly ten additional orders of magnitude. It is hard to say if the cause of this divergent behaviour is due to the rather simple algorithm, the fact that at some pressure the non-relativistic polytrope is no longer applicable, a combination of those two factors, or indeed some error as of yet unaccounted for.

Figure 6b displays no divergence, but it too stops short of reaching $r = 0$. The reason for this is that to assume one radius *and* one mass is to over-constrain the problem. Just as one central density is associated with a pair of values, so too is one radius or one mass. However, the mass and radius are needed at each step of the algorithm. So, for instance, if we posit a radius R, it becomes necessary to solve a set of $N = \frac{R}{\text{integration step size}}$ equations, corresponding to the N values of $M(r = n \cdot dr)$. For this reason we will largely restrict ourselves to algorithms that take the central pressure as an input parameter, and give the mass and radius as output.

We wish to improve and expand upon the result shown in Figure 5, and the first thing we do is to implement two higher-order methods; the explicit Runge-Kutta method known as the 3/8-rule[8], and the fourth order implicit linear multistep Adams–Moulton method[9]. In table 1 we see how the two higher-order methods compare to our original 'naive' approach, and the first things to note is that the two first rows are in good agreement with each other. The step size for the first order central difference method

Table 1: Comparison between the output of our numerical algorithms, for a white dwarf with $P_c = 2.5 \cdot 10^{22}$ Pascal, and using $\gamma = 5/3$.

Algorithm	Radius $[km]$	Mass $[M_\odot]$	Step size $[km]$	Run time $[s]$
Naive	8327	0.78347	0.25	0.14
RK-3/8	8404	0.78350	1.00	0.11
AM-4	8404	0.78350	1.00	6.0
RK-3/8	8406	0.78350	0.02	5.5
AM-4	8300	0.78257	50.0	0.12

was here set to one fourth of the step size of the fourth order Runge-Kutta method because the latter essentially uses the weighted average of four intermediate points to compute the new values - a fact reflected in the similar run time of the two implementations. Furthermore we observe that the most striking difference between the implicit and the explicit fourth order methods is that the implicit method is, given the same step size, approximately 50 times slower. The root cause of this disparity is that the Adams-Moulton method must solve implicit equations of the form

$$y_{n+1} = f(y_{n+1}, r_{n+1}, y_n, r_n, y_{n-1}, r_{n-1}, y_{n-2}, r_{n-2}), \tag{38}$$

whereas the Runge-Kutta method needs only compute expression of the form

$$y_{n+1} = f(y_n, r_n). \tag{39}$$

In light of this, we will do as recommended in[10], and implement both methods. We may then compare the results, and if they differ greatly from one another, that will prompt us to investigate; either revealing an error in implementation, or more seriously, an instability - or some other pathology - in one of the algorithms. But once the comparison has been made, we will prefer the less computationally expensive Runge-Kutta method for those cases where we wish to perform a series of computations.

If we look again at table 1, then on the face of it the naive first order finite difference method seems to be performing quite well. But if we consider Figure 7 - where we have plotted a comparison of the naive and the Runge-Kutta method for pressures approaching zero - we find that the naive algorithm behaves in an oscillatory manner when $P \to 0$.

3.3 Results from the Polytropic Equation of State

Let us compare our numerical solutions of equations (21) and (26) - that is to say, a white dwarf where the electrons are assumed to be non-relativistic, and a white dwarf where the electrons are assumed to be relativistic. In the first case the polytropic exponent is $\gamma = 5/3$, and in the latter it is $\gamma = 4/3$. The most notable feature of Figure 8 is that the polytrope for relativistic electrons converges towards zero pressure comparatively slowly. This strange behaviour is not entirely unexpected, given that

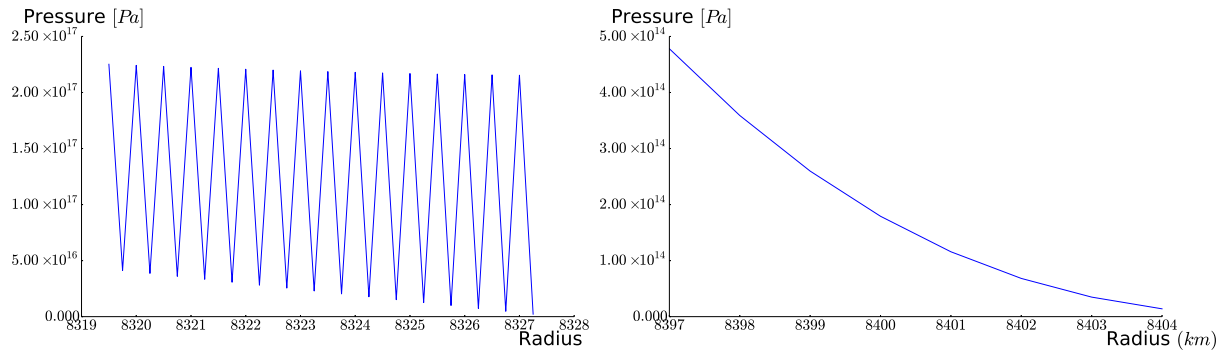

(a) Naive implementation

(b) Runge-Kutta

Figure 7: Zooming in on the termination of the algorithms.

the edge of a white dwarf is unlikely to be well described by an equation of state for relativistic electrons.

The explanation for the peculiar straight line in Figure 9 is less obvious, but the conclusion is clear: For a relativistic white dwarf, the total mass is independent of the central pressure! From this we conclude that there is an upper limit on the mass of relativistic white dwarfs, and that making the relativistic region of a white dwarf denser only makes it smaller, not heavier. This fact may also be derived analytically.[4] It is clear that each polytrope has a limited domain of validity - from Figure 8 we conclude that a relativistic polytrope predicts a radius that is much too large - in fact we had to artificially halt the integration because of how slowly the pressure approached zero - and the fact that the solid line in Figure 9 appears to increase without limit is evidence that the non-relativistic polytrope does not accurately model the denser regions of a white dwarf.

3.4 An Equation of State for Arbitrary Relativity

In the previous subsection we saw some of the differences between the two polytropes, and noted that modeling a white dwarf as purely relativistic, or purely non-relativistic, is problematic. To explore in more detail the conditions in which each polytrope is a valid approximation, we have in Figure 10 plotted the non-relativistic polytrope from equation (21), and the relativistic polytrope from equation (26). In addition, we have a parametric plot of the analytic expression for pressure in a non-interacting electron Fermi gas from equation (19), versus the energy density of non-relativistic neutrons, $n_e m_N c^2 A/Z$, plus the analytic expression for energy density in a non-interacting electron Fermi gas from equation 14c - as functions of the relativity parameter, $u_F = \frac{k_F \hbar}{m_e c}$. As expected, we note that for low values of u_F the $\gamma = 5/3$ plot is equal to, and parallel with, the parametric plot. When $u_F \to 1$ we move out of the the non-relativistic region the parametric curve levels off, and eventually becomes parallel with the $\gamma = 4/3$ curve.

What we want, then, is an equation of state which grows like $\bar{\epsilon}^{5/3}$ in the non-

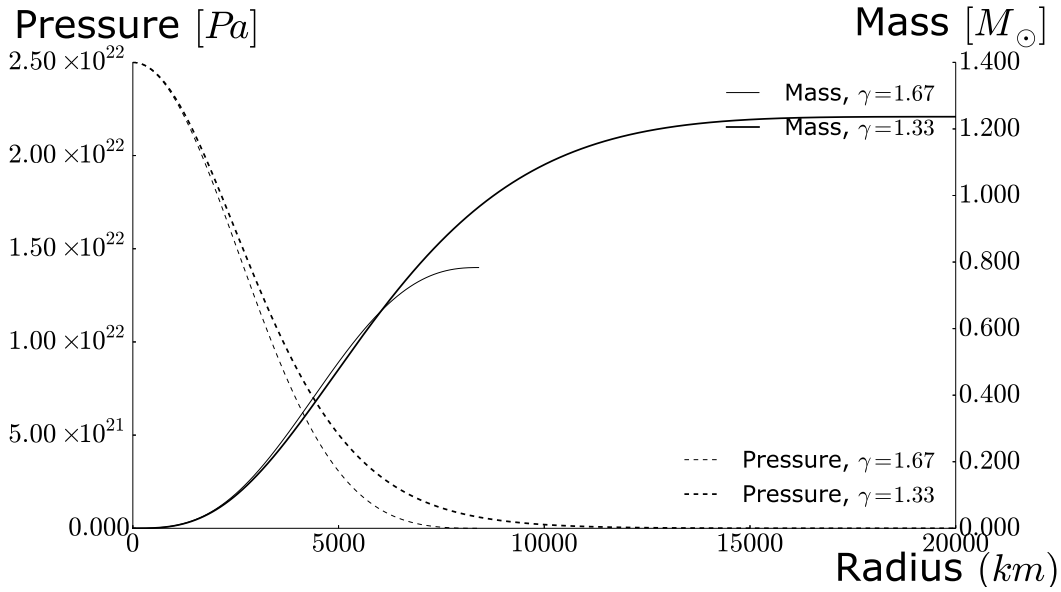

Figure 8: Comparison between white dwarfs with different polytropic exponents.

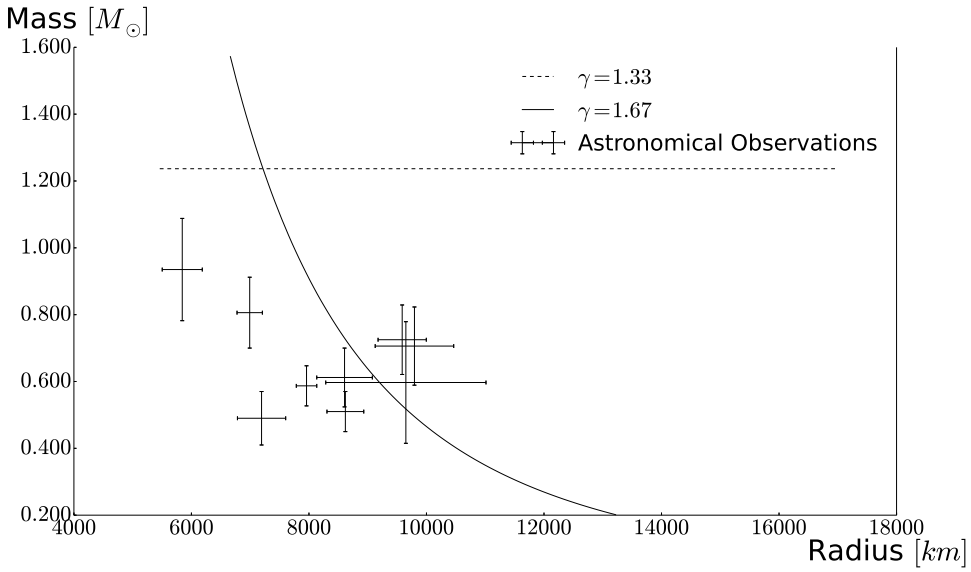

Figure 9: Parametric plots of total mass and radius as functions of central pressure.

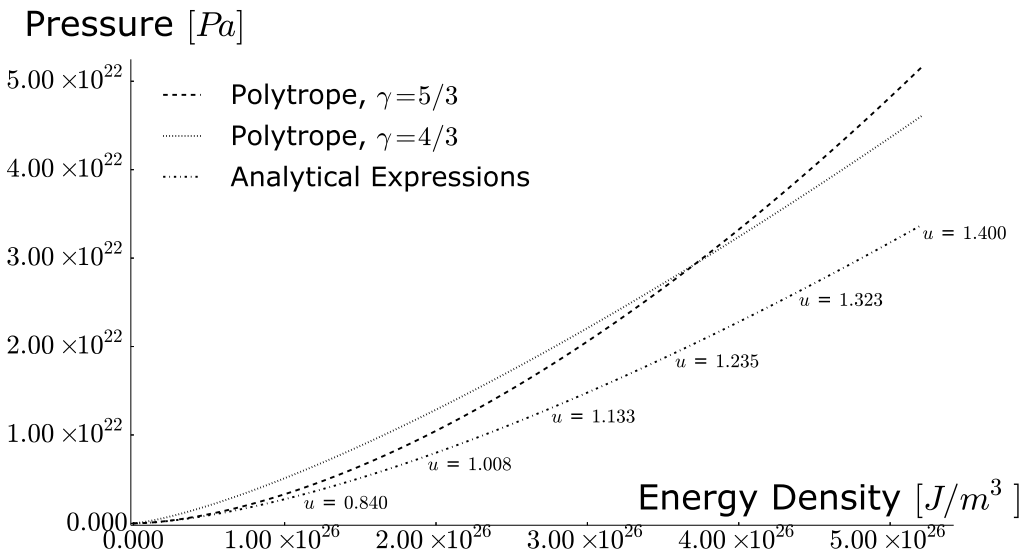

Figure 10: Comparison between three different equations of state.

relativistic regime near the outer edge of the white dwarf, and like $\bar{\epsilon}^{4/3}$ in the relativistic regime closer to the center of the white dwarf. Given a parametric plot such as the one in Figure 10, we can fit an expression for arbitrary relativity of the type

$$\bar{\epsilon} = A_{\mathrm{NR}} \bar{P}^{3/5} + A_{\mathrm{R}} \bar{P}^{3/4}, \tag{40}$$

to the parametric plot by finding suitable coefficients. The choice of these coefficients will depend on the range of pressures and energy densities we attempt to cover with our fit. For very small pressures the coefficient A_{NR} will approach the value predicted by the non-relativistic version of the dimensionless equation for a polytrope, (31),

$$\bar{\epsilon} = \left(1/\bar{K}_{\mathrm{NR}}\right)^{3/5} \bar{P}^{3/5} = 0.06226 \bar{P}^{3/5}, \tag{41}$$

while A_{R} goes to zero. Similarly for large pressures the coefficient A_{R} will approach

$$\bar{\epsilon} = \left(1/\bar{K}_{\mathrm{R}}\right)^{3/4} \bar{P}^{3/4} = 5.385 \bar{P}^{3/4}, \tag{42}$$

while A_{NR} goes to zero. If our curve fit coefficients did not approach these values, that would have been a clear indication that something was amiss.

We showcase a few possibilities in Table 2, where the relativity parameter u ranges from zero to the tabulated values. We also show the pressure corresponding to the tabulated values of the relativity parameter, as predicted by equation 19. These coefficients also depend on the ratio of nucleons to protons, and in computing Table 2 we have taken this ratio to correspond to iron at 56/26. We make a new plot like the one in Figure 9, by using two equations of the arbitrary relativity variety found in equation (40) - one with coefficients computed based on the assumption that $A/Z = 56/26$, and

Table 2: Possible values of the curve fit coefficients, as a function of the maximal value of the relativity parameter on the fitting interval, and with $A/Z = 56/26$.

u	Pressure $[Pa]$	A_{NR}	A_{R}
$\to 0$	$\to 0$	0.06226	0
0.5	$2.79 \cdot 10^{20}$	0.05913	1.217
1.0	$7.41 \cdot 10^{21}$	0.05222	2.466
1.5	$4.59 \cdot 10^{22}$	0.04486	3.394
2.0	$1.60 \cdot 10^{23}$	0.03840	4.043
4.5	$4.71 \cdot 10^{24}$	0.01980	5.385
$\to \infty$	$\to \infty$	0	6.092

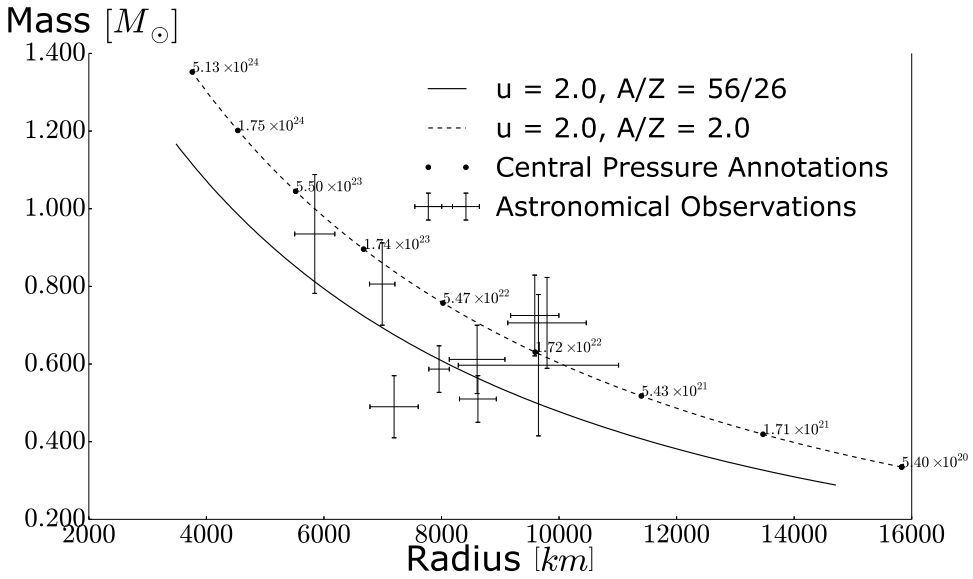

Figure 11: Parametric plot of two different Equations of State for Arbitrary Relativity, combined with astronomical observations by the ESA's Hipparcos satellite.

one with $A/Z = 2$. In both cases the fit of equation (40) onto $(\bar{\epsilon}(u), \bar{P}(u))$ was done with $u \in [0, 2.0]$. When we compare Figure 9 and Figure 11 we see that for our choice of coefficients the equation of state in (40) is a better fit for the astronomical data from the Hipparcos satellite.

3.5 A Piecewise Equation of State

Although our model now seems to be in good agreement with the astronomical data, there is one feature of the relativistic polytrope which is not reproduced in Figure 11, namely the mass limit. Even when we increase the central pressure by several orders of magnitude, the mass shows no sign of any limiting behaviour. We also tried using different sets of the coefficients A_{NR} and A_{R}, corresponding to the intervals $u_F \in [0, 0.5]$, $u_F \in [0, 1.5]$ and, $u_F \in [0, 4.5]$ - the results of which can be seen in Figure 12. In the latter case, the mass grows significantly more slowly as a function of the central pressure, but it still grows without bound.

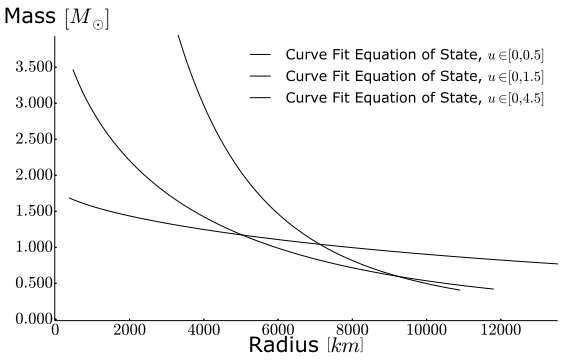

Figure 12: Comparison of three different curve fit EoS,

A curve fit equation of state does a good job of bridging the gap between the relativistic and non-relativistic equations of state, and we can change the coefficients depending on which pressure interval we would like to most accurately represent. However, it can not be correct for both very small and very large pressures, so in an attempt to discern whether the result of a mass limit is purely a feature of the relativistic polytrope, or if it applies to all white dwarfs, we turn to the idea of a piecewise equation of state. As an example to illustrate the concept, we present this function for the energy density

$$\bar{\epsilon} = \begin{cases} 0.05781\bar{P}^{3/5} & & & & & \bar{P} \leq 10^{19} \\ 0.02828\bar{P}^{3/5} & + & 4.349\bar{P}^{3/4} & 10^{19} & \leq & \bar{P} \leq 10^{23} \\ 0.005113\bar{P}^{3/5} & + & 5.549\bar{P}^{3/4} & 10^{23} & \leq & \bar{P} \leq 10^{26} \\ & & 5.657\bar{P}^{3/4} & & & \bar{P} \leq 10^{26} \end{cases}, \tag{43}$$

where the non-relativistic polytrope is used for small pressures, the relativistic polytrope for large pressures, and several equations of state for arbitrary relativity - with coefficients corresponding to some subdivided interval of u_F - for everything in between. The advantage of such a scheme is that for small and large pressures, it deviates less from the true relationship between the energy density and the pressure, compared to using a single equation of state for arbitrary relativity to cover the entire range of pressures.

In Figure 13 we have plotted a parametric plot of total mass and radius as functions of the central pressure, comparing the relativistic polytrope and the curve fit equation of state to an equation of state of the aforementioned piecewise type. In this particular case the piecewise equation of state was stitched together using the relativistic and non-relativistic polytropes, along with nine different curve fit equations of state. It would appear that while the curve fit equation of state works well in most cases, it fails to reproduce the Chandrasekhar limit.

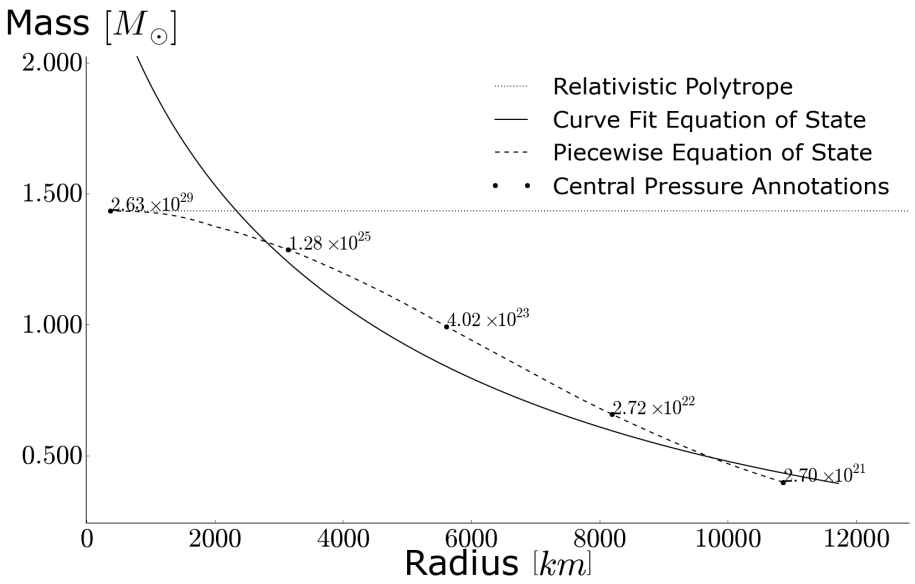

Figure 13: Parametric plot comparing three different kinds of EoS.

4 Neutron Stars

4.1 The Tolman-Oppenheimer-Volkoff Equation

Under the assumption of spherical symmetry it is known that the Schwarzschild metric holds outside the boundary of a star[11]. If we also assume that the star is in hydrostatic equilibrium then the line element may be written as

$$d\tau^2 = -e^{2\nu(r)}dt^2 + e^{2\lambda(r)}dr^2 + r^2 d\theta^2 + r^2 \sin^2\theta \, d\phi^2, \tag{44}$$

where we aim to find functions $\nu(r)$ and $\lambda(r)$ such that equation (44) accurately describes the interior as well as the exterior of the star. In order to determine these functions we will solve the Einstein field equations

$$R_{\mu\nu} - \tfrac{1}{2}R\, g_{\mu\nu} + \Lambda g_{\mu\nu} = -8\pi G T_{\mu\nu}\,, \tag{45}$$

where the pressure and energy density form the stress-energy tensor $T_{\mu\nu}$, the Ricci curvature tensor $R_{\mu\nu}$ and the Ricci curvature scalar R can be computed from the metric, and the cosmological constant Λ may be neglected since it is not relevant at this scale. Furthermore, the field equations may be multiplied by $g^{\mu\nu}$, contracting them and giving us a simpler relation in terms of the curvature scalar and the stress-energy scalar, $R = 8\pi G T^{\mu}_{\mu}$.

In order to do the aforementioned computations of $R_{\mu\nu}$ and R we will first state the Riemann tensor

$$R^{\rho}_{\mu\nu\sigma} \equiv \Gamma^{\rho}_{\mu\sigma,\nu} - \Gamma^{\rho}_{\mu\nu,\sigma} + \Gamma^{\alpha}_{\mu\sigma}\Gamma^{\rho}_{\alpha\nu} - \Gamma^{\alpha}_{\mu\nu}\Gamma^{\rho}_{\alpha\sigma}\,, \tag{46}$$

where $\Gamma^{\rho}_{\mu\nu,\sigma}$ is $\partial_\sigma \Gamma^{\rho}_{\mu\nu}$, and $\Gamma^{\rho}_{\mu\nu}$ is the Christoffel symbol

$$\Gamma^{\rho}_{\mu\nu} \equiv \tfrac{1}{2}g^{\rho\kappa}(g_{\kappa\mu,\nu} + g_{\kappa\nu,\mu} - g_{\mu\nu,\kappa}). \tag{47}$$

The Ricci tensor $R_{\mu\nu}$ is then computed by contracting over two of the indices

$$R_{\mu\nu} \equiv R^{\rho}_{\mu\nu\rho} = \Gamma^{\rho}_{\mu\rho,\nu} - \Gamma^{\rho}_{\mu\nu,\rho} + \Gamma^{\alpha}_{\mu\rho}\Gamma^{\rho}_{\alpha\nu} - \Gamma^{\alpha}_{\mu\nu}\Gamma^{\rho}_{\alpha\rho}\,, \tag{48}$$

which may in turn be contracted by an additional multiplication with the inverse metric $g^{\mu\nu}$, yielding the Ricci scalar $R \equiv g^{\mu\nu}R_{\mu\nu}$.

As an example of how this may be done, I will show the details of the calculation of R_{tt} in the case of the metric in equation (44). In our case we have

$$R_{tt} = R^{\rho}_{tt\rho} = \Gamma^{\rho}_{t\rho,t} - \Gamma^{\rho}_{tt,\rho} + \Gamma^{\alpha}_{t\rho}\Gamma^{\rho}_{\alpha t} - \Gamma^{\alpha}_{tt}\Gamma^{\rho}_{\alpha\rho}\,, \tag{49}$$

and we will do the calculations term by term, starting with

$$\Gamma^{\rho}_{t\rho,t} = \partial_t\left[\tfrac{1}{2}g^{\rho\kappa}(g_{\kappa\rho,t} + g_{\kappa t,\rho} - g_{t\rho,\kappa})\right] = 0, \tag{50}$$

since our assumption of equilibrium - which we shall oft rely on to simplify things - is equivalent to assuming that nothing depends on t. The next term in equation (49) is

$$-\Gamma^{\rho}_{tt,\rho} = -\partial_{\rho}\big[\tfrac{1}{2}g^{\rho\kappa}(g_{\kappa t,t} + g_{\kappa t,t} - g_{tt,\kappa})\big] = \partial_{\rho}\big(\tfrac{1}{2}g^{\rho\kappa}g_{tt,\kappa}\big) \tag{51}$$

where again we have that anything involving a derivative with respect to time drops out, and we are left with a double sum over κ and ρ, which in the most general case contains sixteen (not necessarily unique) terms. However since our metric is diagonal we need only consider $g^{\rho\kappa}$ where $\rho = \kappa$. Additionally we recall from equation (44) that $g_{tt} = -e^{2\nu(r)}$, which means that only $g_{tt,r}$ survives, and we are left with

$$-\Gamma^{\rho}_{tt,\rho} = \partial_{r}\big(\tfrac{1}{2}g^{rr}g_{tt,r}\big) = -\partial_{r}\big(e^{2(\nu-\lambda)}\nu'\big) = -e^{2(\nu-\lambda)}\big[2\nu'(\nu'-\lambda') + \nu''\big], \tag{52}$$

where ν' is $\partial_r\nu$, and the inverse metric g^{rr} is $1/g_{rr}$. The third term in equation (49) is - after letting the derivatives of the metric with respect to time drop out -

$$\Gamma^{\alpha}_{t\rho}\Gamma^{\rho}_{\alpha t} = \tfrac{1}{4}g^{\alpha\kappa}(g_{\kappa t,\rho} - g_{t\rho,\kappa})g^{\rho k}(g_{kt,\alpha} - g_{\alpha t,k}). \tag{53}$$

Again we make use of the fact that our metric is diagonal, which means that at least one of the indices must be t lest all the $g_{\kappa t}$s be zero, and this in turn requires that the matching index in say $g^{\alpha\kappa}$ also must be t. Clearly all the indices can not be t, so the only question is which two indices should be t. After a bit of trial and error one finds

$$\Gamma^{\alpha}_{t\rho}\Gamma^{\rho}_{\alpha t} = \tfrac{1}{4}g^{tt}(g_{tt,\rho} - g_{t\rho,t})g^{\rho k}(g_{kt,t} - g_{tt,k}) = -\tfrac{1}{4}g^{tt}g_{tt,\rho}g^{\rho k}g_{tt,k}, \tag{54}$$

where the only non-zero contribution to the sum is the part where ρ and k are both equal to r, so that

$$-\tfrac{1}{4}g^{tt}g^{rr}(g_{tt,r})^2 = -\tfrac{1}{4}(-e^{-2\nu})(e^{-2\lambda})(-e^{2\nu}2\nu')^2 = e^{2(\nu-\lambda)}\nu'^2. \tag{55}$$

The final term in equation (49) is

$$-\Gamma^{\alpha}_{tt}\Gamma^{\rho}_{\alpha\rho} = -\tfrac{1}{4}g^{\alpha\kappa}(-g_{tt,\kappa})g^{\rho k}(g_{k\alpha,\rho} + g_{k\rho,\alpha} - g_{\alpha\rho,k}), \tag{56}$$

where we first note that $\kappa = r$ is required for $g_{tt,\kappa}$ to be non-zero. Consequently we require $\alpha = r$ to avoid $g^{\alpha\kappa}$ being zero, and we must also have $\rho = k$ to avoid $g^{\rho k}$ being zero. Taken together this gives us

$$\tfrac{1}{4}g^{rr}g_{tt,r}g^{\rho\rho}(g_{\rho r,\rho} + g_{\rho\rho,r} - g_{r\rho,\rho}) = \tfrac{1}{4}g^{rr}g_{tt,r}g^{\rho\rho}g_{\rho\rho,r}, \tag{57}$$

where $g^{\rho\rho}g_{\rho\rho,r} = 2\nu' + 2\lambda' + 2/r + 2/r$, since in this case the indices running over θ and ϕ also contribute to the sum. Inserting this into the above equation gives

$$-\Gamma^{\alpha}_{tt}\Gamma^{\rho}_{\alpha\rho} = -e^{2\nu-\lambda}\nu'(\nu' + \lambda' + \frac{2}{r}). \tag{58}$$

Finally we insert equations (50), (52), (55), and (58) into equation (49), resulting in

$$R_{tt} = e^{2(\nu-\lambda)}\big(\nu'\lambda' - \nu'' - \nu'^2 - \tfrac{2\nu'}{r}\big). \tag{59}$$

Similarly one can calculate

$$R_{rr} = -\nu'\lambda' + \nu'' + \nu'^2 - \tfrac{2\lambda'}{r}, \tag{60a}$$
$$R_{\theta\theta} = (1 + r\nu' - r\lambda')e^{-2\lambda} - 1, \tag{60b}$$
$$R_{\phi\phi} = R_{\theta\theta}\sin^2\theta, \tag{60c}$$

from which we can form the quantity

$$\tfrac{1}{2}(-R_{tt}g^{tt} + R_{rr}g^{rr} + R_{\theta\theta}g^{\theta\theta} + R_{\phi\phi}g^{\phi\phi}) = e^{-2\lambda}\left(\frac{1}{r^2} - \frac{2\lambda'}{r}\right) - \frac{1}{r^2}. \tag{61}$$

The summation in equation (61) can also be performed by taking the Einstein field equations, and inserting them into the stress-energy tensor for a perfect fluid[12]

$$T_{\mu\nu} = Pg_{\mu\nu} + (P + \rho)U_\mu U_\nu, \tag{62}$$

where the four-velocity U^μ is zero for all but the zeroth component. Carrying out the summation leaves us with the relation

$$e^{-2\lambda}\left(\frac{1}{r^2} - \frac{2\lambda'}{r}\right) - \frac{1}{r^2} = -8\pi G\rho, \tag{63}$$

which we may put into a more suggestive form

$$e^{-2\lambda}(1 - 2r\lambda') = \left(r\,e^{-2\lambda}\right)' = 1 - 8\pi G\rho r^2, \tag{64}$$

and integrate to yield

$$e^{-2\lambda} = 1 - \frac{2G}{r}\int_0^r 4\pi\rho(r')r'^2dr' = 1 - \frac{2GM(r)}{r}, \tag{65}$$

where we have defined $M(r) \equiv \int_0^r 4\pi\rho(r')r'^2dr'$.

In a similar manner to how we found equation (63) one may also find the relation

$$e^{-2\lambda}\left(\frac{-1}{r^2} - \frac{2\nu'}{r}\right) + \frac{1}{r^2} = -8\pi GP. \tag{66}$$

Inserting the expression we found for $e^{-2\lambda}$ in equation (65) into equation (66) and rearranging the terms yields

$$\nu' = \left[4\pi GPr + \frac{GM(r)}{r^2}\right]\left[1 - \frac{2GM(r)}{r}\right] \tag{67}$$

We can make further use of the stress-energy tensor for a perfect fluid by enforcing energy-momentum conservation as well as hydrostatic equilibrium, yielding[12]

$$-\partial_\lambda P = (P + \rho)\partial_\lambda \ln(-g_{tt})^{1/2}, \tag{68}$$

and as before only the derivative with respect to r is non-zero, so in our case equation (68) reads

$$-P' = (P+\rho)\nu'. \tag{69}$$

We eliminate ν' from equation (69) by using the expression we found in equation (67) to get the Tolman-Oppenheimer-Volkoff equation

$$P' = -\frac{G\rho M}{r^2}\left[1+\frac{P}{\rho}\right]\left[1+\frac{4\pi r^3 P}{M}\right]\left[1-\frac{2GM}{r}\right]^{-1}, \tag{70}$$

where the explicit dependencies of P, ρ, and M upon r have been suppressed in the name of brevity.

Now that we have this equation we can try to make sense of it in terms of more familiar physics. The star being in equilibrium means that for any given volume element there must be a perfect balance between the outward pressure differential, and the inward gravitational pull

$$-\Delta V P' = \frac{GM_1\Delta M_2}{r^2}. \tag{71}$$

If we consider m_1 to be our $m(r)$ and Δm_2 to be the mass of some small volume element, $\Delta V\rho$, then we can divide out the volume element ΔV to get the Newtonian structure equation

$$P' = -\frac{G\rho M}{r^2}. \tag{72}$$

From (72) we may find (70) if we again consider that $\vec{F} = -V\nabla P = -\nabla U$. So we can view the pressure P as energy per volume, which by the mass energy equivalence means that for large pressures there is a relativistic correction to the density such that $\rho \to \rho + P$, and $m \to m + 4\pi r^3 P$, from which we get

$$P' = -\frac{G}{r^2}(\rho+P)\left(M+4\pi r^3 P\right). \tag{73}$$

To complete the picture consider the coefficient of dr in (44), whose inverse we found in (65). This is the last bracket in (70), which is a general relativistic correction to the radial distance which reflects the fact that space is contracted by the presence of energy, meaning that the star has more space in it than one might expect by simply looking at its radius. Consequently the mass and the gravitational potential are also greater than Newtonian physics would predict.

It is possible to solve the TOV-equation (70) analytically if we assume a constant density $\rho = \rho_0$ throughout the star. Our $m(r)$ then evaluates to $\frac{4\pi}{3}\rho_0 r^3$, so that (70) can be rewritten as

$$P' = -\frac{4\pi G}{3}\frac{(P+\rho_0)(3P+\rho_0)r}{1-8G\pi\rho_0 r^2/3}. \tag{74}$$

Since we expect $P \to 0$ as $r \to R$ we proceed with separation of variables in the following way

$$\int_P^0 \frac{\mathrm{d}P}{(P+\rho_0)(3P+\rho_0)} = G\int_r^R \frac{r\ \mathrm{d}r}{2G\rho_0 r^2 - 3/4\pi}, \tag{75}$$

but note that we could just as well have picked some pressure $P(r{=}0)$ and integrated the other way. Performing the integration gives us

$$\frac{1}{2\rho_0}\log\left(\frac{P+\rho_0}{3P+\rho_0}\right) = \frac{1}{4\rho_0}\log\left(\frac{8G\pi\rho_0 R^2/3 - 1}{8G\pi\rho_0 r^2/3 - 1}\right), \tag{76}$$

and if we let $M = \frac{4\pi}{3}\rho R^3$ denote the total mass of the star then the equation above is equivalent to

$$\frac{P+\rho_0}{3P+\rho_0} = \left(\frac{2GM/R - 1}{2GMr^2/R^3 - 1}\right)^{\frac{1}{2}}, \tag{77}$$

which can be solved for P to yield

$$\frac{P(r)}{\rho_0} = \frac{\left(1-\dfrac{2GM}{R}\right)^{\frac{1}{2}} - \left(1-\dfrac{2GMr^2}{R^3}\right)^{\frac{1}{2}}}{\left(1-\dfrac{2GMr^2}{R^3}\right)^{\frac{1}{2}} - 3\left(1-\dfrac{2GM}{R}\right)^{\frac{1}{2}}}. \tag{78}$$

We can extract a simple result from (78) by evaluating the expression at $r = 0$

$$\frac{P(0)}{\rho_0} = \frac{\left(1-\dfrac{2GM}{R}\right)^{\frac{1}{2}} - 1}{1 - 3\left(1-\dfrac{2GM}{R}\right)^{\frac{1}{2}}}. \tag{79}$$

From Figure 14 we can see that the pressure asymptotically approaches infinity when the parameter $\frac{2GM}{R}$ becomes too large. This tells us that as the mass increases relative to the radius, the pressure P in the core of the star starts to dominate over the density ρ_0, causing the star to become increasingly relativistic. We can find an upper bound for $\frac{2GM}{R}$ either by looking at the plot, or by noting that for positive and real values of P and $\frac{2GM}{R}$ the numerator of (79) is always negative, so we must demand that the denominator also be negative

$$3\left(1-\frac{2GM}{R}\right)^{\frac{1}{2}} > 1 \ \Rightarrow\ \frac{2GM}{R} < \frac{8}{9}. \tag{80}$$

Although this result has here only been proven in the special case of constant density, it can be shown to be true for all stars in a very general way, assuming a non-singular metric and a monotonically decreasing pressure.[13]

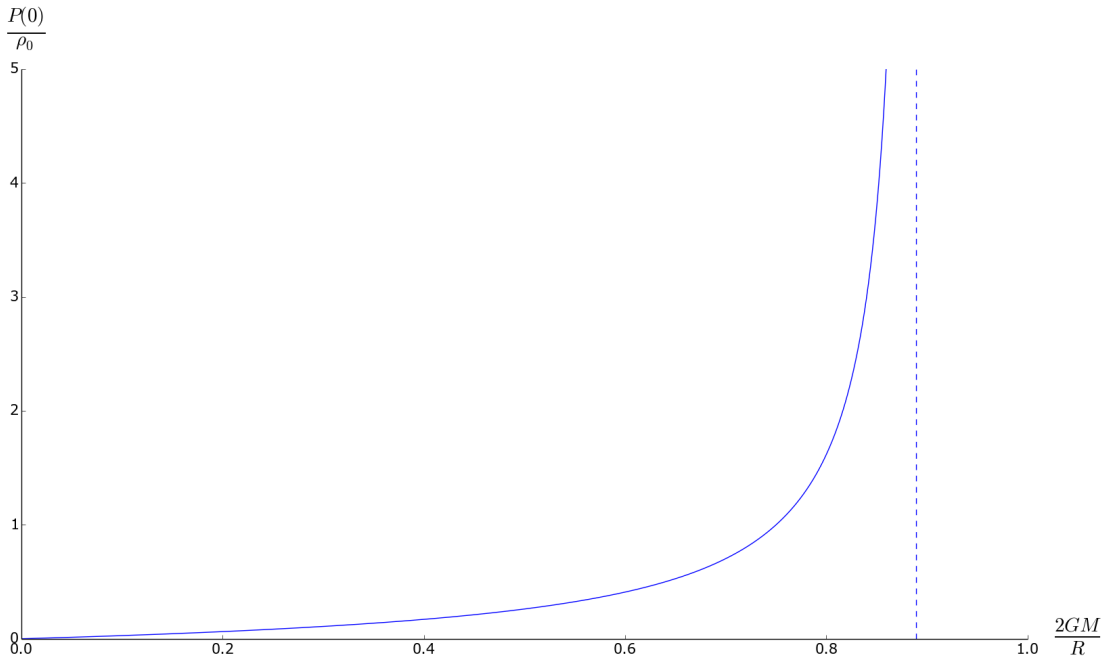

Figure 14: Pressure over density at the center of a sphere of uniform density, as a function of the parameter $\frac{2GM}{R}$.

Given the bound in equation (80), and the relationship between M and R, we can find an upper bound for the radius

$$R < \frac{1}{\sqrt{3\pi G\rho_0}}, \tag{81}$$

and the mass

$$M < \frac{4}{9}\frac{1}{\sqrt{3\pi G^3\rho_0}}, \tag{82}$$

of a star of uniform density. In both cases we see that a greater density implies a smaller star, and that a star of this type can not grow arbitrarily large. Using our newfound knowledge of this upper limit we can pick some reasonable values of $2GM/R$ and plot (78) as a function of r/R. Again we clearly see that as $2GM/R$ approaches $8/9$ the pressure drastically increases. Furthermore we see that in this model the pressure follows a pattern of being nearly level near the core, before decreasing in an approximately linear fashion as the radius increases.

There is another analytical solution to the TOV-equation; if we assume that the neutrons are relativistic, then equations (14) and (18) yield the ultra-relativistic Equation of State for a Fermi gas

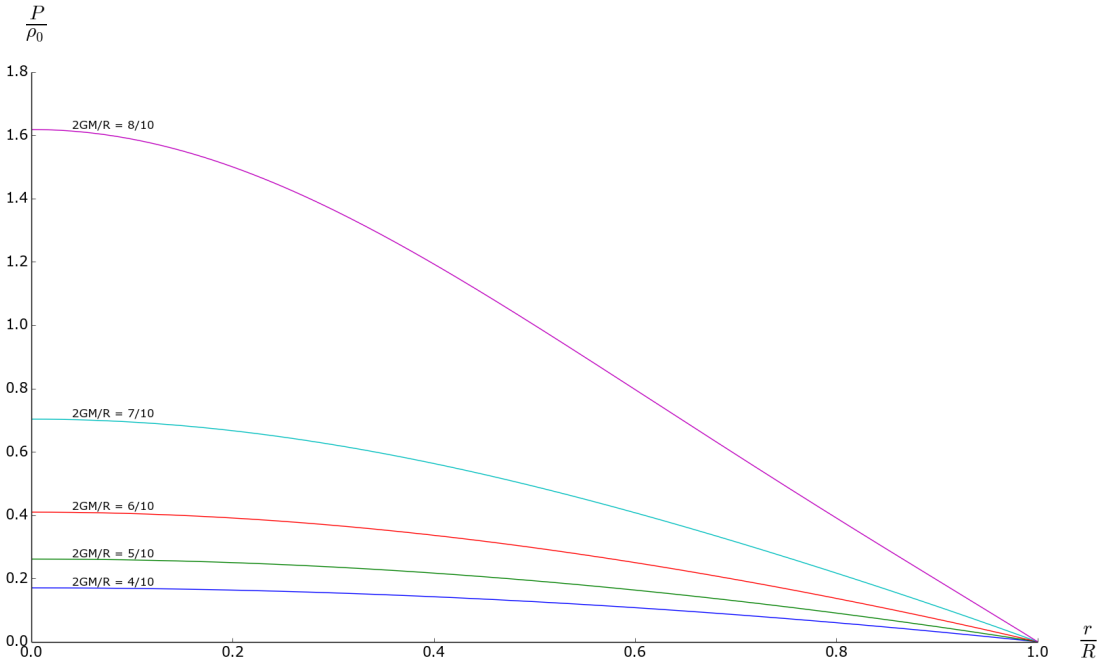

Figure 15: Pressure throughout the inside of a sphere of uniform density, for a few different values of $2GM/R$.

$$P = \frac{\epsilon}{3} = \frac{c^2\rho}{3}, \tag{83}$$

which enables us to re-write the TOV-equation (70) in terms of the density

$$\frac{\rho' r^2}{\rho} = \frac{4GM}{c^2}\left[1 + \frac{4\pi r^3 \rho}{3M}\right]\left[1 - \frac{2GM}{c^2 r}\right]^{-1}. \tag{84}$$

We then make the ansatz that ρ is a simple function of the form

$$\rho = Cr^n, \tag{85}$$

so that the derivative of the pressure at r, and the mass contained within r are

$$\rho' = Cnr^{n-1}, \;\; M = 4\pi\frac{Cr^{3+n}}{(3+n)}, \tag{86}$$

respectively. Inserting these into (84) yields, after some simplification,

$$nr = \frac{4GM}{c^2}\left[1 + \frac{3+n}{3}\right]\left[1 - \frac{2GM}{c^2 r}\right]^{-1}. \tag{87}$$

Multiplying by the inverse of the rightmost bracket and collecting like terms results in

$$r = \frac{2GM}{c^2}\left[\frac{1}{3} - \frac{4}{n}\right] = r^{3+n}\frac{8G\pi C}{c^2(n+3)}\left[\frac{1}{3} - \frac{4}{n}\right]. \tag{88}$$

For this equation to be balanced in powers of r we must have that $n = -2$, which in turn fixes the constant C, and leaves us with the solution

$$\rho = \frac{3c^2}{56\pi G r^2}. \tag{89}$$

The first thing to note is that this solution is not physically realizable - it goes to infinity for small values of r, and only asymptotically approaches zero for large values of r. It is not surprising that the solution behaves poorly in the non-relativistic regime, but given the assumption of an ultra-relativistic equation of state, one might have thought that it would accurately describe the high density regime. Unfortunately, our simple ansatz left no room for finding monotonically decreasing solutions that did not have this problem of divergence. Additionally, there are no adjustable parameters other than the radius. So if we were to take equation (89) seriously, the implication would be that there is exactly one completely unique solution, and that we should expect all neutron stars to be exactly the same.

When moving to the numerical solution, we expect some of the characteristics of these analytical solutions to feature. Specifically, the pressure should behave as in Figure 15 for small r, given that the very core of the star experiences the greatest pressure, and thus the smallest density gradient.

4.2 Numerical Results

We proceed in much the same way as we did for white dwarfs - first using a polytropic equation of state, with $\gamma = 5/3$, to model a neutron star; and then finding an equation of state for arbitrary relativity by curve fitting a function of the form

$$\bar{\epsilon}(\bar{P}) = A_{NR}\bar{P}^{3/5} + A_R\bar{P} \tag{90}$$

to a parametric plot of the pressure, from equation 19, versus the analytic expression for energy density, from equation (14c) - with the neutron mass m_N replacing the electron mass m_e, so that the equations describe a neutron Fermi gas. Again we emphasise that the coefficients in equation (90) will depend on the range of the input parameter, u_F, and present a few choice values in Table 3. In either case, the assumption that we can write the energy density as a function of pressure lets us rewrite the TOV-equation (70) in terms of the pressure. If we also introduce the constant

$$\delta = \frac{4\pi\epsilon_0}{M_\odot c^2}, \tag{91}$$

we can put the TOV-equation into dimensionless form

$$P' = -\frac{\alpha\bar{\epsilon}(\bar{P})\bar{M}}{r^2}\left[1 + \frac{\bar{P}}{\bar{\epsilon}(\bar{P})}\right]\left[1 + \delta r^3\frac{\bar{P}}{\bar{M}}\right]\left[1 - \frac{2\bar{M}R_0}{r}\right]^{-1}. \tag{92}$$

Table 3: Possible values of the curve fit coefficients, as a function of the maximal value of the relativity parameter on the fitting interval.

$\frac{k_F\hbar}{m_N c}$	Pressure $[\epsilon_0]$	A_{NR}	A_R
0.5	0.0058	2.625	2.603
1.0	0.15	2.613	2.670
1.5	1.0	2.583	2.736
2.0	3.3	2.539	2.789
2.5	8.6	2.487	2.831

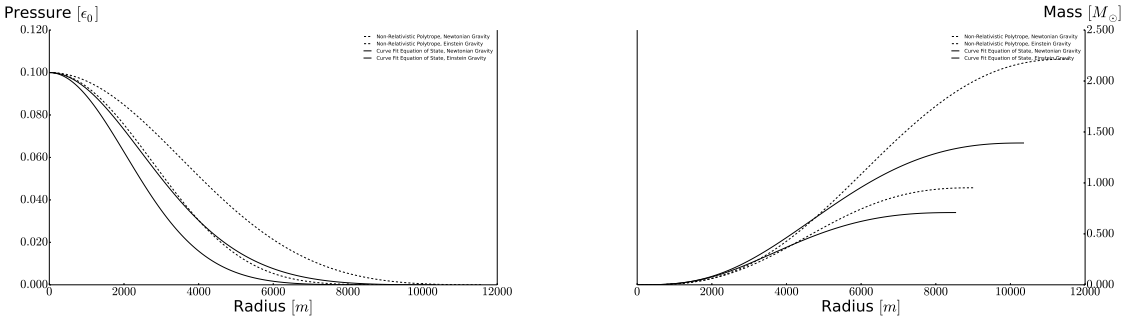

(a) Pressure as a function of radius.

(b) Mass as a function of radius.

Figure 16: Comparison between pressure and mass as functions of radius for four different combinations of equation of state and gravitational model.

Looking at Figure 16 we see that though they are not identical, the shape of the graphs are very similar in all four cases. In particular, the pressure of a non-relativistic polytrope under the effects of Einstein gravity is very nearly identical to the pressure of the curve fit equation of state under Newtonian gravity. On the other hand it is clear from looking at the mass plots that Newtonian gravity is not a good approximation, as it leads to a mass estimate which is twice as large as the general relativistic prediction.

And to better pinpoint for which central pressures the polytropic approximation fails, we look at the parametric plot in Figure 17, where although there is no one clear point of departure, we feel confident in saying that the deviation is small for central pressures below $0.001\epsilon_0$, and significant for central pressures in excess of $0.01\epsilon_0$. We can make this more precise by comparing the equation of state in (90) with the non-relativistic polytrope for a neutron star in equation 21

$$\bar{\epsilon}(\bar{P}) = 2.613\bar{P}^{3/5} + 2.670\bar{P}, \tag{93}$$

$$\bar{\epsilon}(\bar{P}) = \left(\frac{\bar{P}}{\bar{K}}\right)^{3/5} = 2.627\bar{P}^{3/5}, \tag{94}$$

and calculating when the central pressure predicted by the polytrope deviates by more than, say, 10%. We find that this happens when the central pressure exceeds $0.0033\epsilon_0$.

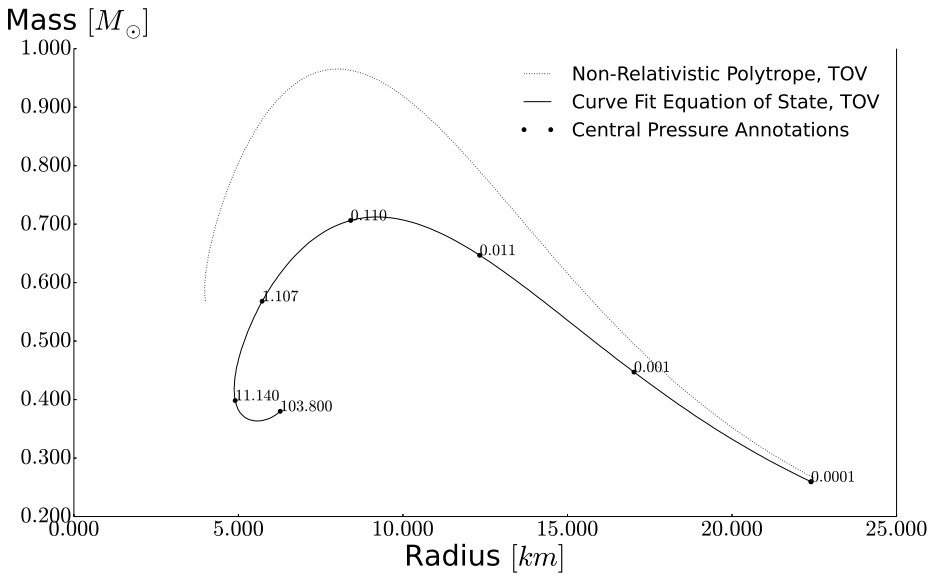

Figure 17: Parametric plot of Neutron star masses and radii for two different EoS, one a curve fit for arbitrary relativity, and the other a non-relativistic polytrope.

Figure 17 also highlights that, to good approximation, there is a logarithmic relationship between the central pressure and the arc length of the curve. Similarly, the mass is proportional to the logarithm of the central pressure, and the radius is inversely proportional logarithm of the central pressure. Finally there is the striking fact that there appears to be a maximum mass, and in contrast to what we found for white dwarfs the maximum mass corresponds to a single radius - solutions with smaller radius than the radius corresponding to the maximum mass are less massive. Figure 18 implies that the cause of this discrepancy is that our model for white dwarfs was at the time not fully relativistic. Moreover, our result for the maximum mass is significantly smaller than more realistic estimates.[4]

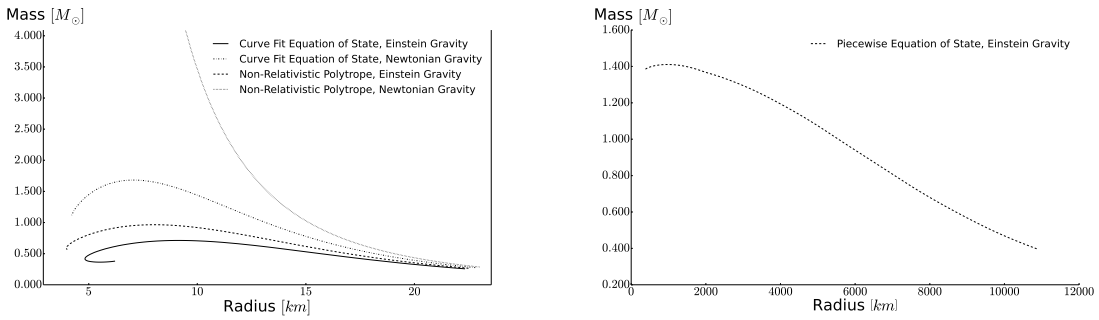

Figure 18: Comparison between parametric plots of mass as a function of radius for neutron stars with four different combinations of equation of state and gravitational model, and one plot of a white dwarf with general relativistic corrections and a piecewise equation of state

4.3 Limiting Mass and Stability

In Figures 13 and 17 we have seen that our models predict a limiting mass of white dwarfs and neutron stars. However, one can imagine a situation where more mass is imparted to, say, a neutron star by accretion from its binary partner[14] - thus pushing it above the mass limit. Since our model does not admit the existence of such a star, we conclude that a star pushed above the limiting mass no longer conforms to the assumptions underpinning our model - that the star is a non-interacting zero temperature Fermi gas in hydrostatic equilibrium. If the latter assumption isn't true then the star must be in the process of collapsing or expanding. Dropping the first assumption and allowing for interactions introduces, among other things, the possibility of reactions that change the constituents of the star. Specifically, we know that in the case of white dwarfs it is possible for protons to capture electrons, thus becoming neutrons. Indeed, this neutronization is the conventional explanation for what happens when a white dwarf collapses into a neutron star[4] - though it is worth noting that another likely fate of a white dwarf gaining mass through accretion is to explode in a nova, dispersing some of the material involved[15].

There is one argument we can make based on our model, based on the idea that an equilibrium can be either stable or unstable. Some equilibriums are stable against perturbations, while others are not. The canonical example of an unstable equilibrium is a ball perched on top of a hill - untouched it will forever remain on that one flat spot, but give it the slightest push and it will tumble down the hill. We will show how the configurations to the left of the maximum mass in Figure 17 are unstable against gravitational collapse. Such a star would have smaller radius and greater density than the corresponding star to the right of the mass limit. To make the argument more clear let us look at the simplified graph in Figure 19, where we have sketched a parametrization in terms of mass and central pressure rather than mass and radius. Imagine a neutron star with greater radius - thus per the central pressure annotations in Figure 17 it is a neutron star with smaller central pressure - and with the benefit of foreknowledge dub it S for stable. Then imagine that it is compressed for some reason or the other. This new configuration, $\bar{S}$, has greater density and an increased degeneracy pressure when compared to S, but it has the same mass. If $\bar{S}$ had more mass, it would be in hydrostatic equilibrium and fit on the line as the star S'. This tells us that in the compressed star $\bar{S}$ the degeneracy pressure can not be weaker than gravity - otherwise the more massive star S', which experiences an equal or greater gravitational self-attraction $\bar{S}$ and the same pressure, would not be in equilibrium. Thus the balance of forces in $\bar{S}$ is such that degeneracy pressure will cause the star would bounce back after being compressed, returning it to S.

For the star sagaciously named U the situation is different. If the star is compressed then the density and thus the degeneracy pressure increases, as was the case for S. However, when comparing $\bar{U}$ to the equilibrium configuration U' with the same pressure one finds that gravity is comparatively stronger in $\bar{U}$. Thus the overall situation is reversed when compared to $\bar{S}$ - instead of degeneracy pressure acting to return $\bar{U}$ to U,

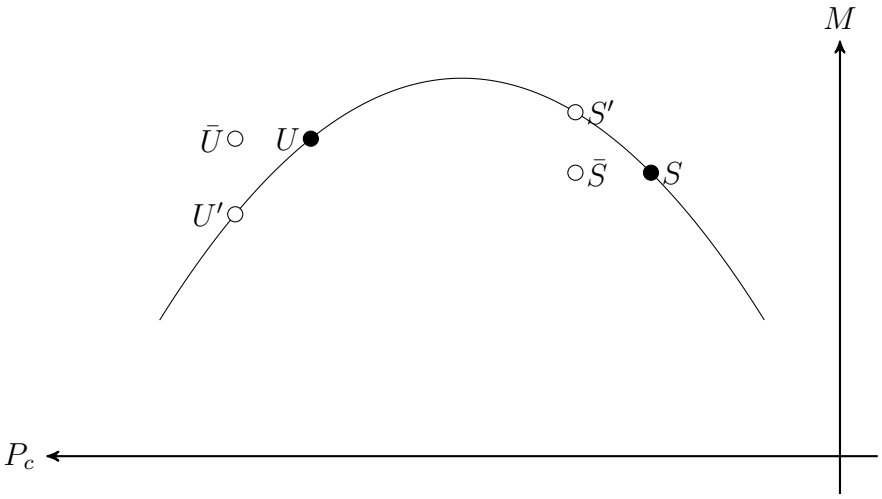

Figure 19: A schematical representation of the relationship between the total mass M, and the central pressure P_c of neutron stars. Configurations to the left of the maximum mass are in an unstable equilibrium.

gravity acts to further compress $\bar{U}$.

5 Summary and Conclusions

We have modeled white dwarfs and neutron stars as a non-interacting Fermi gas at zero temperature, supported against gravitational collapse by electron and neutron degeneracy pressure, respectively. With a non-relativistic polytropic equation of state, $P = K\epsilon^{5/3}$, this model produced white dwarf radii and masses which fit observational data for low mass white dwarfs. Using a relativistic polytropic equation of state, $P = K\epsilon^{4/3}$, reproduced the Chandrasekhar limit, but gave *no* predictions for low mass white dwarfs. This showed that a simple polytropic equation of state worked well in the regime it was made for, but that the difference in conditions within a white dwarf are too large to be wholly described by such a simple equation of state.

We curve fit an equation of state of the form $P = A_{\mathrm{NR}}\epsilon^{5/3} + A_{\mathrm{R}}\epsilon^{4/3}$ to a plot of the analytical values of pressure and density, resulting in better agreement with the observational data. However, this curve fit equation of state did not exhibit the limiting mass predicted by the Chandrasekhar limit, so to further improve our model we introduced a piecewise equation of state, composed of several curve fit equations of state - each covering a limited range of pressures and densities. The result of this added complexity was a plot which showed agreement with observational data, and exhibited the same limiting mass predicted by Chandrasekhar. This shows that modeling a white dwarf as a non-interacting Fermi gas at zero temperature is a good approximation.

In contrast, our model of neutron stars significantly undershoots observational data on neutron star masses, to the point where the heaviest neutron star is twice as light as

the heaviest white dwarf. That's not to say that our model isn't useful - the comparisons we made between different approximations to the same equations of state show that there are significant differences between polytropic and curve fit equations of state, and our comparisons between neutron stars under the effect of Newtonian gravity on the one hand and Einstein gravity on the other make it clear that neutron stars are objects best described in the context of a general relativistic theory.

For both types of compact stars discussed herein we found a maximum mass, above which we should not expect to find stars described by our model. Taken together with the fact that configurations with central densities equal to or greater than the maximum mass can be shown to be in an unstable equilibrium, it seems likely that any star above the maximum mass will undergo some kind of transformation - either shedding mass, or collapsing.

Finally, we showed that the simplest explicit integrator of ordinary differential equations - the Euler method - grows unstable when the pressure approaches zero. We did not observe any such behaviour from the 4th order explicit Runge-Kutta method, nor from the 4th order implicit Adams-Moulton method. For similar step sizes the implicit method was roughly fifty times slower than the explicit method.

6 Where Do We Go From Here?

The fact that the maximum mass of a neutron star, as predicted by our non-interacting model, fell short of the observational data whereas the predicted radii and masses of the white dwarfs were in good agreement indicates that we can not ignore interactions if we wish to accurately model a neutron star. Therefore an obvious next step would be to find some way to incorporate nucleon-nucleon interactions in our model. This is a difficult task, in part because quantum field theory is a complicated machinery, but also because neutron stars are the only place in the universe where neutrons are packed so closely together. On the other hand this makes it a very interesting field of study - since such dense configurations of matter are not well understood, we can use observational data from neutron stars to check whether our models are correct.

Additionally we considered our neutron stars to be made exclusively out of neutrons, but in reality there is an admixture of neutrons, protons, and electrons in most of the star - all of whom must obey the requirement of global electric neutrality. **??**. Closer to the core there may be exotic hadrons and degenerate quark matter. In the case of white dwarfs we briefly touched on the fact that their composition varies from star to star - some are richer in heavier nuclei, while others have a comparatively greater proportion of light nuclei. Either of these possibilities would be worth exploring in greater detail.

On the computational side of things we might have spent more time comparing different algorithms - in particular it would have been interesting to find out more about the conditions under which an algorithm for solving the TOV-equation exhibits instability. One might ask if it is primarily the order and step size of the algorithm which is to blame, or if there is there some pathological equation of state which may -

for instance - make the 4th order Runge-Kutta methods unstable.

Finally there is the question of rotation and magnetic fields - conservation of angular momentum and magnetic flux cause neutron stars to spin up to 716 times per second[16], and have magnetic fields up to 17 orders of magnitude greater than the magnetic field of the earth. The spin acts to further stabilise the star against gravitational collapse, and the magnetic field has implications for the structure of the star.

Appendices

A Pressure of a non-interacting Fermi gas

From the first law of thermodynamics, $dE = dQ - PdV$, we get the relation

$$P = -\frac{\partial E}{\partial V}, \tag{95}$$

if we assume that the temperature is constant. We may recast this relation in terms of the energy density and the number density, and then use the chain rule to expand the terms

$$P = -\frac{\partial(N\epsilon/n)}{\partial(N/n)} = -\frac{\partial(N\epsilon/n)/\partial n}{\partial(N/n)/\partial n} = -\frac{(\partial N/\partial n)\epsilon/n + N(\partial(\epsilon/n)/\partial n)}{\frac{1}{n}(\partial N/\partial n) - N/n^2}. \tag{96}$$

This expression can be simplified by noting that since N/n is a constant, the partial derivative $\partial N/\partial n$ is zero, and thus

$$P = n^2\frac{\partial(\epsilon/n)}{\partial n} = n\frac{d\epsilon}{dn} - \epsilon. \tag{97}$$

Since we are assuming that the electrons are non-relativistic, it follows that the heavier nucleons are also non-relativistic. Therefore we may consider the energy density of the nucleons to be completely dominated by their rest energy, $\epsilon_N = n_e m_N \frac{A}{Z}c^2$, and treat ϵ_N as a constant. Under this assumption we have that

$$P = n_e^2\frac{\partial(\epsilon_e/n_e + n_e m_N \frac{A}{Z}c^2/n_e)}{\partial n_e} = n_e^2\frac{\partial(\epsilon_e/n_e)}{\partial n_e}, \tag{98}$$

which, if we plug in the integral form of equation (14), becomes

$$P = n_e^2\frac{m_e^4c^5}{\pi^2\hbar^3}\frac{\partial}{\partial n_e}\left[\frac{1}{n_e}\int(u^2+1)^{1/2}u^2du\right]. \tag{99}$$

This expression looks rather thorny, but we will show that it can be put into a nice form. Applying the product rule, and ignoring the the numerical factors, yields

$$P \propto -\frac{1}{n_e^2}\int(u^2+1)^{1/2}u^2du + \frac{1}{n_e}\frac{\partial}{\partial n_e}\int(u^2+1)^{1/2}u^2du. \tag{100}$$

Since u is related to n_e through k_F, there exists a substitution $U = \left(n_e^{2/3}\chi^2+1\right)^{1/2}\frac{\chi^3}{3}$, where $\chi = \frac{\hbar}{m_e c}(3\pi^2)^{1/3}$, such that

$$\int(u^2+1)^{1/2}u^2du = \int Udn_e = Un_e - \int ndU. \tag{101}$$

Hence

$$P \propto -\frac{1}{n_e^2}\left(Un_e - \int ndU\right) + \frac{1}{n_e}\frac{\partial}{\partial n_e}\int U dn_e, \tag{102}$$

which by the fundamental theorem of calculus simplifies to

$$P \propto \frac{1}{n_e^2}\int n_e dU. \tag{103}$$

Restoring numerical factors and reverting the transformation gives us the result

$$P = \frac{m_e^4 c^5}{3\pi^2\hbar^3}\int_0^{u_F} (u^2+1)^{-1/2}u^4 du. \tag{104}$$

B Python Scripts

To save space I have not included all the code. Notably there are no plotting routines included, and the script for finding the coefficients for the Arbitrary Relativity equation of state was left out.

compactStar.py

```
from constants import *
from HipparcusGaia import hipparcus

import time
import math
import numpy as np
from scipy.optimize import fsolve
from scipy.optimize import curve_fit as fit

'''
This script works by first creating an object in the class "Star", and
   then calling one of the integration methods defined within the class.
   For example the sequence of lines

NeutronAE = Star(star='neutron',a_rel=True,g_rel=True)
R, M, P = NeutronAE.RK38()

first creates a class object and assigns it the name "NeutronAE", uses
   the class method integrator RK38 on it, which creates vectors with
   radius, mass, and pressures of the given "Star" object and assigns the
    output of that method to the variables R, M, P.
'''

class Star(object):
    '''Parameters of the star, and of the integration algorithm'''
    def __init__(self, star='neutron', a_rel=True, piecewise=False,
                 g_rel=True, gamma=5.0/3.0, pressure=0, AR_default=2):
        self.star = star              #Type of star, white or neutron
        self.a_rel = a_rel            #a_rel = False -> Polytrope EoS,
           a_rel = True -> Arbitraty Relativity EoS
        self.AR_default= AR_default #Controls which coefficients are used
            in the AR EoS for white dwarfs
        self.piecewise = piecewise  #Piecewise EoS
        self.g_rel = g_rel            #General Relativity
        self.gamma = gamma                #Polytropic index
        self.nu = 1.0/gamma

        if self.star == 'white':
            self.dr = 1000.0          #stepsize in meters
            self.Pc = 2.5*10**22      #loosely based on average density
            self.A = 52.0             #number of protons in Iron
            self.Z = 26.0             #number of neutron is Iron
            self.RMAX = 2.0*10**7     #maximum radius
            '''These values are based on curve fitting to a parametric
```

```
            plot of (e(u),P(u))
             with u in the interval {0,relParam},
             and relParam = [0.5, 1.0, 1.5, 2.0, 2.5, 4.5]
             Generated by ArRelWD.py'''
        self.AR = [[0.05490861, 1.1299978],[0.04848809, 2.28982439],
                   [0.04165437, 3.15205892],[0.03565586, 3.75509996],
                   [0.03069424, 4.17828088],[0.01837873, 5.00110446]]

        '''Corresponding values of P(u)'''
        self.Pcut = [2.79*10**20/epsilon0, 7.41*10**21/epsilon0,
                     4.59*10**22/epsilon0, 1.60*10**23/epsilon0,
                     4.14*10**23/epsilon0, 4.71*10**24/epsilon0]

        '''...with u in the interval {relParam[n],relParam[n+1]}...
        relParam = [0.1, 0.2, 0.35, 0.5, 1.0, 1.5, 2.5, 4.5, 7.0,
            10.0]
             Generated by ArRelWDPiecewise.py'''
        self.AR2 = [[0.05728564, 0.39502537],[0.05616687,
            0.79267173],
                   [0.05429222, 1.25990663],[0.04791268, 2.36464381],
                   [0.03923298, 3.38943866],[0.02828418, 4.34864880],
                   [0.01646565, 5.09516187],[0.00921769, 5.42361918],
                   [0.00511335, 5.55941348]]

        self.Pcut2 = [10**17, 3.1*10**18, 4.9*10**19, 2.79*10**20,
            7.41*10**21,
                      4.59*10**22, 4.14*10**23, 4.71*10**24,
                         2.83*10**25, 1.19*10**26]

        self.Anr, self.Ar = self.AR[self.AR_default]
                    #TODO: look into making Anr and Ar depend on the
                        pressure
                    #probably better to implement in the solver
                    #DONE - but the current implementation through
                        eps() is slow

    elif star == 'neutron':
        self.dr=10.0
        self.Pc = 2.5*10**34        #epsilon0 = 5.46*10^35, reference
            value
        self.A = 26.0
        self.Z = 26.0
        self.RMAX = 10**5/2
        self.AR = [[2.62527618, 2.60312049],
                   [2.61292102, 2.66981139],[2.58286878, 2.73583722],
                   [2.53879713, 2.78944920],[2.48665957, 2.83058394]]
                    #relativity parameter <= 0.5, 1.0,  1.5, 2.0, 2.5
        self.cutoff =           [0.0058, 0.15, 1.0, 3.3, 8.6]
        self.Anr, self.Ar = self.AR[0]

    '''Polytropic constant of proportionality'''
    self.KWDNR = hbar**2/(mE*15*np.pi**2)*((self.Z*3*np.pi**2)/(self.
```

```
            A*mN*c**2))**(5.0/3.0)
        self.KWDUR = hbar*c/(12*np.pi**2)*(3*np.pi**2*self.Z/(mN*c*c*self
            .A))**(4.0/3.0)
        if gamma == 5.0/3.0 and star == 'white':
            self.K = self.KWDNR

        elif gamma == 4.0/3.0 and star == 'white':
            self.K = self.KWDUR

        elif gamma == 5.0/3.0 and star == 'neutron':
            self.K = hbar**2/(mN*15*np.pi**2)*((self.Z*3*np.pi**2)/(self.
                A*mN*c**2))**gamma

        elif gamma == 1.0:
            self.K = 1.0/3.0

        if a_rel == True:
            self.K, self.gamma, self.nu = 1.0, 1.0, 1.0

        '''Scaling and non-dimensionalisation'''
        self.alpha = R0/(self.K**self.nu*epsilon0**(1.0-1.0/self.gamma))
        self.beta = 4*np.pi/(mS*c*c)*(epsilon0/self.K)**(1.0/self.gamma)
        self.delta = 4*np.pi/(mS*c*c)*epsilon0

        '''Default pressure value, or input pressure value'''
        if pressure != 0:
            self.Pc = pressure

        self.P0 = self.Pc/epsilon0

    '''Differential Equations'''
    def dPdr(self,r,M,P):
        if self.a_rel == 0:                    #Assuming polytrope
            if self.g_rel == 1:              #Ignoring general relativistic
                effects
                return -self.alpha*M*P**self.nu/r**2*(1+P**(1-self.nu)*R0
                    /self.alpha)*(1+self.delta*P/M*r**3)/(1-2*M*R0/r)
            elif self.g_rel == 0:
                return -self.alpha*M*P**self.nu/r**2

        elif self.a_rel == 1:
            if self.g_rel == 1:
                return -self.alpha*M*self.eps(P)/r**2*(1+P/self.eps(P))
                    *(1+self.delta*P/M*r**3)/(1-2*M*R0/r)
            elif self.g_rel == 0:
                return -self.alpha*M*self.eps(P)/r**2

    def eps(self,P):
        if self.piecewise == False:
            if self.star == 'neutron':
                return self.Anr*P**(3.0/5.0) + self.Ar*P
```

```
            elif self.star == 'white':
                return self.Anr*P**(3.0/5.0) + self.Ar*P**(3.0/4.0)

        elif self.piecewise == True:
            if self.star == 'neutron':
                def anal_p(t, P):
                    return P - (1.0/8.0 * ((2*t**3 - 3*t)*(1+t**2)**0.5 +
                        3*np.arcsinh(t)))
                def anal_e(t):
                        return 3.0/8.0 * ((2*t**3 + t)*(1+t**2)**0.5 - np
                            .arcsinh(t))
                return anal_e(fsolve(anal_p, P**0.20, args=(P)))

            elif self.star == 'white':
                if P <= self.Pcut2[0]/epsilon0:
                    return (self.KWDNR*epsilon0**(5.0/3.0-1.0))
                        **(-3.0/5.0)*P**(3.0/5.0)
                elif self.Pcut2[0]/epsilon0 < P and P <= self.Pcut2[-1]/
                    epsilon0:
                    for i in range(len(self.Pcut2[:-1])):
                        if self.Pcut2[i]/epsilon0 < P and P <= self.Pcut2
                            [i+1]/epsilon0:
                             self.Anr, self.Ar = self.AR2[i]
                    return self.Anr*P**(3.0/5.0) + self.Ar*P**(3.0/4.0)
                elif self.Pcut2[-1]/epsilon0 < P:
                    return (self.KWDUR*epsilon0**(4.0/3.0-1.0))
                        **(-3.0/4.0)*P**(3.0/4.0)

    def dMdr(self,r,P):
        if self.a_rel == 0:
            return self.beta*r**2*P**self.nu
        if self.a_rel == 1:
            return self.beta*r**2*self.eps(P)

    '''Differential Equation solvers'''
    def RK38(self):
        R,M,P = self.AM1(RMAX=self.dr)
        dr = self.dr
        r = dr
        while r < self.RMAX and P[-1] > 0:
            '''Runge-Kutta 3/8'''
            try:
                p1 = self.dPdr(r,M[-1],P[-1])
                m1 = self.dMdr(r,P[-1])
                p2 = self.dPdr(r+dr/3,M[-1]+dr*m1/3,P[-1]+dr*p1/3)
                m2 = self.dMdr(r+dr/3,P[-1]+dr*p1/3)
                p3 = self.dPdr(r+dr*2/3,M[-1]+dr*(-m1/3 +m2),P[-1]+dr*(-
                    p1/3 +p2))
                m3 = self.dMdr(r+dr*2/3,P[-1]+dr*(-p1/3 +p2))
                p4 = self.dPdr(r+dr,M[-1]+dr*(m1 - m2 + m3),P[-1]+dr*(p1
                    - p2 + p3))
                m4 = self.dMdr(r+dr,P[-1]+dr*(p1 - p2 + p3))
```

```
                M.append(M[-1] + dr/8*(m1+3*m2+3*m3+m4))
                P.append(P[-1] + dr/8*(p1+3*p2+3*p3+p4))
                r = r + dr
                R.append(r)

            except ValueError:
                break

        R,M,P = cut(R,M,P)
        return R,M,P

    def BEuler(self,p,r,M1,P1):
        return p - P1 - self.dr*self.dPdr(r,M1+self.dr*self.dMdr(r,p),p)

    def Trapezoidal(self,p,r,M1,P1):
        return p - P1 - self.dr/2.0*(self.dPdr(r,M1+self.dr*self.dMdr(r,p
            ),p) + self.dPdr(r,M1,P1))

    def AM_S3_P(self,p,r,M1,M2,M3,P1,P2,P3):
        '''Intermediate Pressure Computation in AM4'''
        return p - P1 - self.dr/24.0*(9*self.dPdr(r,M1
                + self.AM_S3_M(p,r,P1,P2,P3),p)
                + 19*self.dPdr(r-self.dr,M1,P1)
                - 5*self.dPdr(r-2*self.dr,M2,P2)
                + self.dPdr(r-3*self.dr,M3,P3))

    def AM_S3_M(self,p,r,P1,P2,P3):
        '''Intermediate Mass Computation in AM4'''
        return self.dr/24.0*(9*self.dMdr(r,p)
                + 19*self.dMdr(r-self.dr,P1)
                - 5*self.dMdr(r-2*self.dr,P2)
                + self.dMdr(r-3*self.dr,P3))

    def AM1(self,RMAX):
        '''Adams-Moulton - backward Euler, s=0'''
        R,M,P = [0], [0], [self.P0]
        r, PP = 0, P[-1]                                    #PP is the
            Pressure Predictor
        while r < RMAX and P[-1] > 0:
            r = r + self.dr
            #Note the float      - np.float64 slows down RK38 by 15, and
                AM4 by 2
            P.append(float(fsolve(self.BEuler, PP, args=(r,M[-1],P[-1])))
                )
            M.append(M[-1] + self.dr*self.dMdr(r,P[-1]))
            R.append(r)
            PP = P[-1] + self.dr*self.dPdr(R[-1],M[-1],P[-1])    #
                Prediction for the next iteration
        R,M,P = cut(R,M,P)
        return R, M ,P
```

```
    def AM2(self,RMAX):
        '''Adams-Moulton - Trapezoidal, s=1'''
        R, M, P = self.AM1(RMAX=self.dr)                #using the lower
            order method for the first step
        r = self.dr
        while r < RMAX and P[-1] > 0:
            r = r + self.dr
            #predictor
            PP = P[-1] + self.dr*self.dPdr(r-self.dr,M[-1],P[-1])
            #corrector
            P.append(fsolve(self.Trapezoidal, PP, args=(r,M[-1],P[-1])))
            M.append(M[-1] + self.dr*self.dMdr(r,P[-1]))
            R.append(r)
        R,M,P = cut(R,M,P)
        return R, M ,P

    def AM4(self):
        '''Adams-Moulton - 4th order, s=3'''
        R, M, P = self.AM2(RMAX=3*self.dr)      #using the lower order
            methods for the first steps
        r = 3*self.dr
        while r < self.RMAX and P[-1] > 0:
            r = r + self.dr
            #predictor
            PP = P[-1] + self.dr*self.dPdr(r-self.dr,M[-1],P[-1])
            #corrector
            P.append(fsolve(self.AM_S3_P, PP, args=(r,M[-1],M[-2],M[-3],P
                [-1],P[-2],P[-3])))
            M.append(M[-1] + self.AM_S3_M(P[-1],r,P[-2],P[-3],P[-4]))
            R.append(r)
        R,M,P = cut(R,M,P)
        return R, M ,P

'''Helper functions'''

def cut(R,M,P):
    #cuts away unphysical values of P, along with the corresponding r and
        M
        while P[-1]     < 0 or math.isnan(P[-1]) == True:
                R,M,P = R[0:-1],M[0:-1],P[0:-1]
        return R,M,P

def parametricRandM(star,iterations):
    #computes R, M, P for increasing values of the central pressure
    radius, mass, pressure = [],[],[]
    for i in range(iterations):          #195+30
        star.P0=star.P0*1.08
        R, M, P = star.RK38()
        radius.append(R[-1]/1000.0)
        mass.append(M[-1])
        pressure.append(P[0])
    return radius, mass, pressure
```

HipparcusGaia.py Observational data from the Hipparcus satellite

```
hipparcus = ([[0.612,0.088],[1.237,0.068]],
             [[0.597,0.182],[1.387,0.196]],
             [[0.587,0.060],[1.144,0.025]],
             [[0.490,0.080],[1.034,0.059]],
             [[0.935,0.153],[0.840,0.049]],
             [[0.706,0.117],[1.408,0.096]],
             [[0.510,0.060],[1.239,0.045]],
             [[0.806,0.106],[1.005,0.031]],
             [[0.725,0.104],[1.378,0.059]])
```

constants.py

```
c       =   299792458                   # m/s
hbar    =   1.0545718*10**(-34) # J s
G       =   6.674*10**(-11)             # m^3 kg^-1 s^-2
eV      =   1.6021766*10**(-19) # J
mP      =   1.673*10**(-27)             # kg
mN      =   1.673*10**(-27)             # kg
mE      =   9.109*10**(-31)             # kg
mS      =   1.9891*10**30               # kg
rS      =   6.957*10**8         # m

R0      =  G*mS/c**2
epsilon0 = mN**4*c**5/(3*3.14159265359**2*hbar**3)
```

ArRelWE.py Finds the coefficients for the Arbitrary Relativity equation of state.

```
from scipy.optimize import curve_fit as fit
import numpy as np
from constants import *
A, Z = 52, 26 #52, 26
epsilon0 = mE**4*c**5/(3*np.pi**2*hbar**3)
const    = 3*np.pi**2*Z/(mN*c**2*A)
def ArRel(x,Anr,Ar):                           #energy density as a
    function of pressure
        return (Anr)*x**(3.0/5.0) + (Ar)*x**(3.0/4.0)

def p(t):
        return 1.0/8.0 * ((2*t**3 - 3*t)*(1+t**2)**0.5 + 3*np.arcsinh(t))

def e(t):
        return 3.0/8.0 * ((2*t**3 + t)*(1+t**2)**0.5 - np.arcsinh(t)) +
           mN/mE*A/Z*t**3

def pRel(energydensity):
    return hbar*c/(12*np.pi**2)*(const*energydensity)**(4.0/3.0)

def pNonRel(energydensity):
    return hbar**2/(15*np.pi**2*mE)*(const*energydensity)**(5.0/3.0)

'''Plotting routine'''
import matplotlib.pyplot as plt
```

```
import matplotlib as mpl

fig , ax = plt.subplots(1,1)

I = [0.5, 1.0, 1.5, 2.0, 2.5, 4.5]
imax = 100000
T = np.linspace(0.001,I[-1],imax)        #t is the relativity parameter k*
    hbar/mc
P = np.array([p(t) for t in T])*(mE/mN)**4       #xdata
E = np.array([e(t) for t in T])*(mE/mN)**4       #ydata
s = int(len(P)*2.0/5.0)                                  #use to zoom in
ax.plot(P[:s],E[:s])
for i in I:

        popt, pcov = fit(ArRel, P[:int(imax*i/I[-1])], E[:int(imax*i/I
            [-1])])
        print 'Dimensionless pressure = {:.3}'.format(epsilon0*(mN/mE)
            **4*P[int(len(P)*i/I[-1])-1])
        print popt
        #E_fit = np.array([ArRel(p,popt[0],popt[1],popt[2]) for p in P])
        E_fit = np.array([ArRel(p,popt[0],popt[1]) for p in P])
        ax.plot(P[:s],E_fit[:s])
        ax.text(P[:s][-1],E_fit[:s][-1],r'$\frac{k_F \hbar}{m_e c}$ = %s'
            %i)

ax.get_xaxis().get_major_formatter().set_scientific(False)
ax.yaxis.set_major_formatter(mpl.ticker.ScalarFormatter(useMathText=True,
    useOffset=False))
ax.spines['right'].set_color('none')
ax.spines['top'].set_color('none')
ax.xaxis.set_ticks_position('bottom')
ax.spines['bottom'].set_position(('data',0))
ax.yaxis.set_ticks_position('left')
ax.spines['left'].set_position(('data',0))
#labels and their positions
ax.set_xlabel(r'pressure')
ax.set_ylabel(r'energy density')
ax.xaxis.set_label_coords(1.05, 0.04)
ax.yaxis.set_label_coords(0.005, 1.01)
#text size
ax.xaxis.label.set_size(30)
ax.yaxis.label.set_size(30)
ax.tick_params(axis='both', which='major', labelsize=15)
ax.tick_params(axis='both', which='minor', labelsize=12)

plt.show()
```

References

[1]E. Öpik, "The densities of visual binary stars", Astrophysical Journal **44**, 292 (1916).

[2]A. S. Eddington, *Stars and atoms* (Clarendon Press, Oxford, 1927).

[3]J. B. Zirker, *Journey from the center of the sun* (Princeton University Press, Princeton, 2002).

[4]N. K. Glendenning, *Compact stars*, Second Edition (Springer Verlag, New York, New York, 2000).

[5]D. J. Griffiths, *Introduction to quantum mechanics*, Second Edition (Pearson Education, Upper Saddle River, New Jersey, 2005), p. 219.

[6]H. P. Langtangen, and G. K. Pedersen, *Scaling of differential equations*, URL: https://hplgit.github.io/scaling-book/doc/pub/book/pdf/scaling-book-4screen-sol.pdf (Springer Verlag, June 2016), p. 18.

[7]P.-E. Tremblay, N. Gentile-Fusillo, R. Raddi, S. Jordan, C. Besson, B. T. Gänsicke, S. G. Parsons, D. Koester, T. Marsh, R. Bohlin, J. Kalirai, and S. Deustua, "The Gaia DR1 mass-radius relation for white dwarfs", Montly Notices of the Royal Astronomical Society **465**, p. 8, 2849–2861 (2017).

[8]M. W. Kutta, "Beitrag zur näherungsweisen integration totaler differentialgleichungen", Zeitschrift für Mathematik und Physik **46**, 435–453 (1901).

[9]E. Hairer, S. P. Nørsett, and G. Wanner, *Solving ordinary differential equations i: nonstiff problems* ().

[10]N. J. Higham, *Accuracy and stability of numerical algorithms*, Second Edition (Society for Industrial and Applied Mathematics, Philadelphia, 1993), p. 27.

[11]J. B. Hartle, *Gravity: an introduction to einstein's general relativity*, First Edition (Addison Wesley, San Francisco, CA, 2002), p. 186.

[12]S. Weinberg, *Gravitation and cosmology: principles and applications of the general theory of relativity* (Wiley, New York, NY, 1972), pp. 127–128.

[13]S. Weinberg, *Gravitation and cosmology: principles and applications of the general theory of relativity* (Wiley, New York, NY, 1972), p. 334.

[14]D. Bhattacharya, and E. van den Heuvel, "Formation and evolution of binary and millisecond radio pulsars", Physics Reports **203**, 1–124 (1991).

[15]S. Starrfield, C. Iliadis, F. X. Timmes, W. R. Hix, W. D. Arnett, C. Meakin, and W. M. Sparks, "Theoretical studies of accretion of matter onto white dwarfs and the single degenerate scenario for supernovae of Type Ia", Bulletin of the Astronomical Society of India **40**, 419 (2012).

[16]J. W. T. Hessels, S. M. Ransom, I. H. Stairs, P. C. C. Freire, V. M. Kaspi, and F. Camilo, "A radio pulsar spinning at 716 hz", Science **311**, 1901–1904 (2006).